Chapter 8
Proteome Analysis Identified the PPARγ Ligand 15d-PGJ2 as a Novel Drug Inhibiting Melanoma Progression and Interfering with Tumor-Stroma Interaction

Verena Paulitschke, Silke Gruber, Elisabeth Hofstätter, Verena Haudek-Prinz, Philipp Klepeisz, Nikolaus Schicher, Constanze Jonak, Peter Petzelbauer, Hubert Pehamberger, Christopher Gerner and Rainer Kunstfeld

Abstract Peroxisome proliferator-activated receptors (PPARs) have been originally thought to be restricted to lipid metabolism or glucose homeostasis. Recently, evidence is growing that PPARγ ligands have inhibitory effects on tumor growth.

To shed light on the potential therapeutic effects on melanoma we tested a panel of PPAR agonists on their ability to block tumor proliferation *in vitro*. Whereas ciglitazone, troglitazone and WY14643 showed moderate effects on proliferation, 15d-PGJ2 displayed profound anti-tumor activity on four different melanoma cell lines tested.

Additionally, 15d-PGJ2 inhibited proliferation of tumor-associated fibroblasts and tube formation of endothelial cells. 15d-PGJ2 induced the tumor suppressor gene p21, a G_2/M arrest and inhibited tumor cell migration.

Shot gun proteome analysis in addition to 2D-gel electrophoresis and immunoprecipitation of A375 melanoma cells suggested that 15d-PGJ2 might exert its effects via modification and/or downregulation of Hsp-90 (heat shock protein 90) and several chaperones. Applying the recently established CPL/MUW database with a panel of defined classification signatures, we demonstrated a regulation of proteins involved in metastasis, transport or protein synthesis including paxillin, angio-associated migratory cell protein or matrix metalloproteinase-2 as confirmed by zymography. Our data revealed for the first time a profound effect of the single compound 15d-PGJ2 on melanoma cells in addition to the tumor-associated microenvironment suggesting synergistic therapeutic efficiency.

PLoS ONE: Research Article, published 25 Sep 2012 10.1371/journal.pone.0046103

V. Paulitschke (✉) · S. Gruber · E. Hofstätter · N. Schicher · C. Jonak · P. Petzelbauer · H. Pehamberger · R. Kunstfeld
Dept. of Dermatology, Medical University of Vienna, Vienna, Austria
e-mail: rainer.kunstfeld@meduniwien.ac.at

V. Haudek-Prinz · P. Klepeisz · C. Gerner
Dept. of Medicine I, Medical University of Vienna, Vienna, Austria

A. Reichle (ed.), *Evolution-adjusted Tumor Pathophysiology,*
DOI 10.1007/978-94-007-6866-6_8,

Introduction

Defining novel treatment options of melanoma is still a challenge and the identification of new agents is vital due to the increasing incidence and poor prognosis [1, 2]. For any novel drug, many obstacles have to be overcome from target identification to clinical testing of therapeutics. Therefore, drugs already approved for the treatment of other diseases but potentially applicable in melanoma are of high interest [1].

There is increasing evidence that the peroxisome proliferator-activated receptor-γ (PPARγ)-binding ligands, may be effective for the treatment of melanoma [1] and other tumors [3].

PPARs are ligand-activated transcription factors of the nuclear hormone receptor superfamily comprising three subtypes: PPARα, PPARγ, and PPARδ/β and are characterized by distinct functions, ligand specificities and tissue distribution [4]. The role of these receptors has been considered originally to be restricted to lipid and lipoprotein metabolism, glucose homeostasis and cellular differentiation [5].

PPARγ was demonstrated to regulate diverse cellular and neoplastic processes such as proliferation [6], differentiation [7] and apoptosis [8]. The anti-tumor effect of PPARγ activation is exerted by the induction of cell cycle arrest rather than by induction of apoptosis [9, 10]. In addition, the inhibition of endothelial cell migration by PPARγ ligands has been described, bolstering the anti-angiogenic activity of PPAR ligands [11, 12].

The PPARγ specific agonists 15-deoxy-Δ12,14 prostaglandin J2 (15d-PGJ2), troglitazone, and rosiglitazone inhibited cell proliferation in four melanoma cell lines dose-dependently, whereas a specific agonist of peroxisome proliferator-activated receptor alpha (WY-14643) did not exert this effect [9]. Ciglitazone, a selective PPARγ ligand, was shown to inhibit the proliferation of the A375 as well as of the WM35 melanoma cell line [13].

Several PPAR ligands are interesting candidates for melanoma therapy. Thiazolidinediones (TZD), ciglitazone and troglitazone are high affinity synthetic ligands. In contrast, 15d-PGJ2 is a low-affinity endogenous ligand for PPARγ and known to be a potent inducer of heme oxygenase 1 (HO-1). The three high affinity ligands directly regulate cyclin D1 and p21 and the multi-functional protein ß-catenin [14, 15]. The latter observation implies that PPARγ ligands may be able to interfere with the metastatic process [16].

Here we present a comprehensive study assessing the anti-tumorigenic effects of a panel of PPARα and PPARγ agonists on a variety of melanoma cell lines. The PPARγ agonists ciglitazone, troglitazone and 15d-PGJ2 and the PPARα ligand WY-14643 were tested on four melanoma cell lines (A375, M24met, 1205Lu and MelJuso) to generalize our findings. In addition to direct effects on cancer cells, PPARγ agonists were tested on the influence on cells of the tumor microenvironment such as endothelial cells and melanoma associated fibroblasts.

To further investigate molecular mechanisms of drug action we made use of the proteome profiling methods shot gun analysis and 2D-gel electrophoresis. Applying the recently established CPL/MUW proteomics database [17, 18] we were able to detect protein alterations independently supporting the present functional data.

Our study indicates that 15d-PGJ2 is a potent anti-tumorigenic compound by interfering with melanoma cell proliferation, metastasis and additionally affecting the melanoma associated stroma.

Results

15d-PGJ2 Inhibits Cell Proliferation More Efficiently Than Other PPAR Ligands Via Cell Cycle Arrest And p53 Regulation

We investigated the anti-proliferative effects of PPARγ ligands ciglitazone, troglitazone and 15d-PGJ2 and the PPARα ligand WY-14643 on four melanoma cell lines (A375, M24met, 1205Lu and MelJuso). As determined by MTS proliferation assays, the IC_{50} of 15d-PGJ2 was in a range between 22–38 μM after 48 h of treatment (Table 8.1). In contrast the IC_{50} of the PPARγ agonists ciglitazone and troglitazone could not be reached with the highest dose of 100 μM tested on A375, M24met and MelJuso melanoma cell lines. The selective PPARα agonist WY-14643 showed no growth inhibitory effect (Table 8.1). Thus, among the tested PPARγ agonists 15d-PGJ2 was found most efficient.

Next we investigated the anti-proliferative effects on human umbilical vein endothelial cells (HUVECs) and skin-derived fibroblasts of healthy donors. The IC_{50} of isolated HUVECs was 85, of LECs 70.84, suggesting a restriction of 15d-PGJ2 efficiency to malignant cells (Table 8.1).

In contrast to normal fibroblasts such as NHDF with an IC50 of 127.70, the melanoma associated fibroblasts of four different patients revealed to be more sensitive upon15d-PGJ2 treatment (IC_{50} range: 44–68 μM).

The PPARγ expression in the melanoma cell lines (A375, M24met, 1205Lu, MelJuso), in HUVECs, normal fibroblasts (NHDFs) and primary melanoma associated fibroblasts (MP9, MP10, MP11, MCM16 fibroblasts) was confirmed via Western blotting (Fig. 8.1a).

We selected 15d-PGJ2, the most potent PPARγ agonist for further investigations.

We analyzed cell cycle alterations mediated by 15d-PGJ2 in A375, M24met and 1205Lu melanoma cell lines. In all melanoma cell lines 15d-PGJ2 induced a G_2/M arrest. Treatment of cells with 15 μM 15d-PGJ2 triggered cell cycle arrest in the G_2/M phase from 18–63 %, from 12–32 % in and from 5–26 % in A375 (Fig. 8.1b), in M24met (Fig. 8.1c) and in 1205Lu cells (Fig. 8.1d), respectively.

Since p21 is known to induce S-phase or G_2/M arrest [19–21], we tested our cells for p21 induction after 15d-PGJ2 treatment. Indeed, 15d-PGJ2 treatment dose-dependently induced upregulation of p21 in A375, M24met and 1205Lu at low micromolar concentrations (Fig. 8.2a). Additionally, 15d-PGJ2 induced p53 expression and/or phosphorylation in A375, M24met and 1205Lu melanoma cell lines (Fig. 8.2b).

Table 8.1 IC50 of cells treated with PPAR ligands

Cell line	PPAR ligand	IC50 (μM)
A375 (melanoma cell line)	Ciglitazone	> 100 (1436)
	Troglitazone	> 100 (2584)
	15d-PGJ2	*23.4*
	WY-14643	> 800 (14394)
M24met	Ciglitazone	> 100 (2913)
	Troglitazone	>100 (1574)
	15d-PGJ2	*25.12*
	WY-14643	674.4
1205Lu	Ciglitazone	100.9
	Troglitazone	46.09
	15d-PGJ2	*21.97*
	WY-14643	380.9
MelJuso	Ciglitazone	> 100 (2,721e + 007)
	Troglitazone	> 100 (580.4)
	15d-PGJ2	*37.45*
	WY-14643	791.5
HUVEC (endothelial cells)	Ciglitazone	> 100 (16242)
	Troglitazone	> 100 (1615)
	15d-PGJ2	*85.23, 83.7 (2nd isolated cell)*
	WY-14643	> 800 (835)
LEC (lymphatic endothelial cells)	15d-PGJ2	*70.84*
Cell line	*PPAR ligand*	*IC50 (μM)*
NHDF (normal skin fibroblasts)	15d-PGJ2	*127,70*
TF (old)	15d-PGJ2	*92,78*
MP9 fibroblasts	15d-PGJ2	*46,92*
MP10 fibrosblasts	15d-PGJ2	*44,40*
MP11 fibroblasts	15d-PGJ2	*54,40*
MCM16 fibroblasts	15d-PGJ2	*68,22*

15d-PGJ2 is superior to other PPAR ligands in inhibiting growth of melanoma cell lines, endothelial cells and of tumor associated fibroblasts superior to normal fibroblasts.Cell viability and proliferation assay. The IC50 is calculated of three independent experiments. IC50 of melanoma cells A375, M24met, 1205Lu, MelJuso and endothelial cells (HUVECs) treated with ciglitazone, troglitazone, 15d-PGJ2 and WY-14643, lymphatic endothelial cells (LECs), normal fibroblasts (NHDF) and tumor-associated fibroblasts treated with 15d-PGJ2

15d-PGJ2 Exerts Inhibitory Effects on Tumor Cell Migration, Angiogenesis and Lymphangiogenesis

Impact of 15d-PGJ2 on melanoma cell migration was investigated using a Matrigel invasion chamber assay. 15d-PGJ2 inhibited M24met melanoma cell migration in a dose-dependent manner and inhibited tumor cell migration at a concentration of 5 μM after 48 h (Fig. 8.3a). At a concentration of 25 μM migration is totally abolished as demonstrated in the M24met and A375 melanoma cell lines (Fig. 8.3a, b). The percentage of transmigrated cells is quantified by Axiovion software.

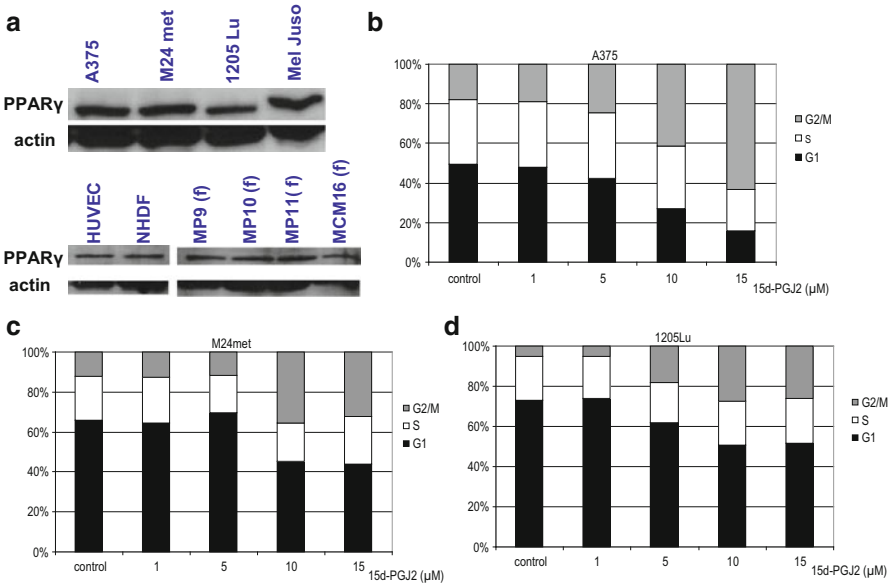

Fig. 8.1 PPARγ receptor expression and G2/M arrest induction by 15d-PGJ2. **a** receptor expression on A375, M24met, 1205Lu, MelJuso melanoma cells and HUVECs as well as fibroblasts NHDF and melanoma associated fibroblasts. (f): fibroblasts **b**, **c** and **d**: Cell cycle analysis by flow cytometry using propidium iodide- stained on A375, M24met and 1205Lu. Cells were treated for 24 h with different concentrations of 15d-PGJ2. Three independent experiments were pooled and analyzed as a combined data set

Inhibition of angiogenesis was demonstrated by a dose dependent disturbance of tube formation of HUVECs after 12 and 24 h (Fig. 8.3c, d). Inhibition of lymphangiogenesis was indicated repeating these experiments with lymphatic endothelial cells (LECs) (Fig. 8.3e, f). Here pronounced effects could be observed already at a concentration of 5 μM 15d-PGJ2. Tube formation was quantified using the Cell Profiler Software Package and calcein staining was used to demonstrate the vitality of the cells.

Shot Gun Analysis for Characterisation of the Acting Profile of 15d-PGJ2

Shot gun analysis of nuclear and cytoplasmic fractions of untreated A375 cells resulted in the identification of a total of 2,250 proteins. Proteins were classified according to gene ontology terms accessible via uniprot. Shot gun analysis of 15d-PGJ2-treated A375 cells revealed 136 proteins which displayed increased peptide counts compared to the control (Table 8.2, 8.3). Amongst these we identified proteins involved in the lipid metabolism (protein count/peptide count = 7/7) such

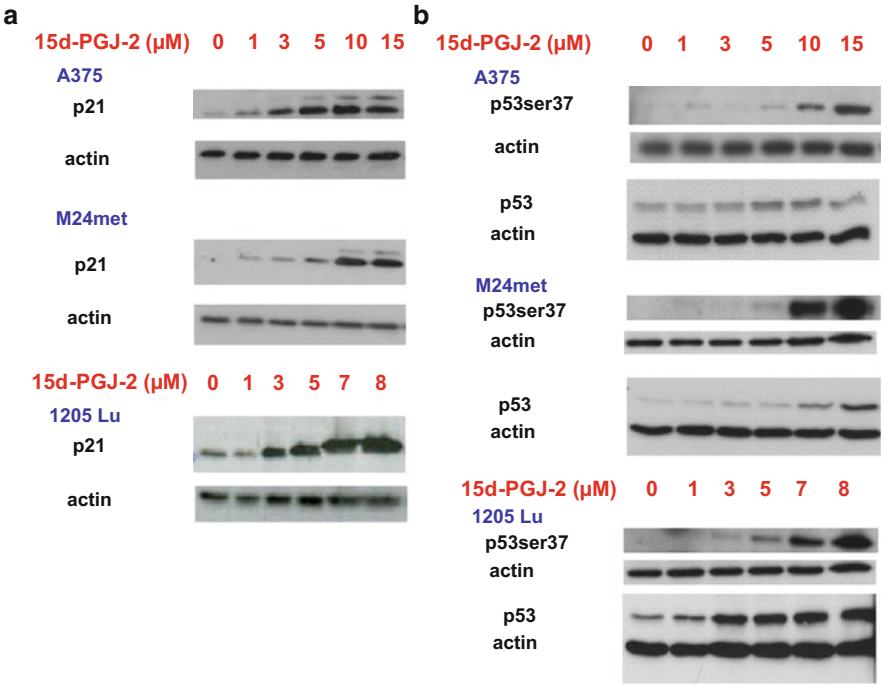

Fig. 8.2 15d-PGJ2 induces p21 expression and p53, p53ser37. **a** 15d-PGJ2 leads to an induction of p21. Immunoblotting of p21 after 48 h of 15d-PGJ2 treatment with indicated concentrations. **b** Immunoblotting of p 53 and p 53ser37 after 48 h of 15d-PGJ2 treatment with indicated concentrations

as thromboxane-A synthase, adipophilin, perilipin or apolipoprotein A-I (Table 8.2, 8.3) [22, 23]. Additionally, we detected the induction of HO-1 by 15d-PGJ2 (Table 8.2, 8.3) [24]. As depicted in Fig. 8.4a and b proteins/peptides involved in DNA repair mechanisms (5/7) such as MSH3, telomeric repeat-binding factor 2 or MMS2 (Table 8.2, 8.3), phosphorylation by ATM/ATR upon DNA damage (13/21), transport (21/26), mRNA processing (13/21), protein synthesis (5/12), replication (10/13) and transcription (8/8) were upregulated. In accordance with our data proteins involved in cell cycle such as the lymphokine-activated killer T-cell-originated protein kinase or with anti-proliferative effects such as nodal-modulator 1 revealed to be induced (Table 8.2, 8.3) (Uniprot). Proteins indicating a cellular stress response such as sterile 20/oxidant stress-response kinase 1 or growth arrest and DNA damage-inducible protein GADD45 beta were regulated as well (Table 8.2, 8.3) (Uniprot). The DNA repair proteins MMS2, MSH3, MSH6, MSH2, MLH1 and the upregulation of basigin at 1 μM and nodal at 15 μM was confirmed by Western blot analysis (Fig. 8.5).

Furthermore, several proteins related to angiogenesis such as angio-associated migratory cell protein, to cell cycle such as cyclin – A1 and H, to metastasis, to cell migration and to interaction with the extracellular matrix (ECM) such as paxillin or syntenin-1 and to proliferation such as PCNA (proliferating cell nuclear antigen)

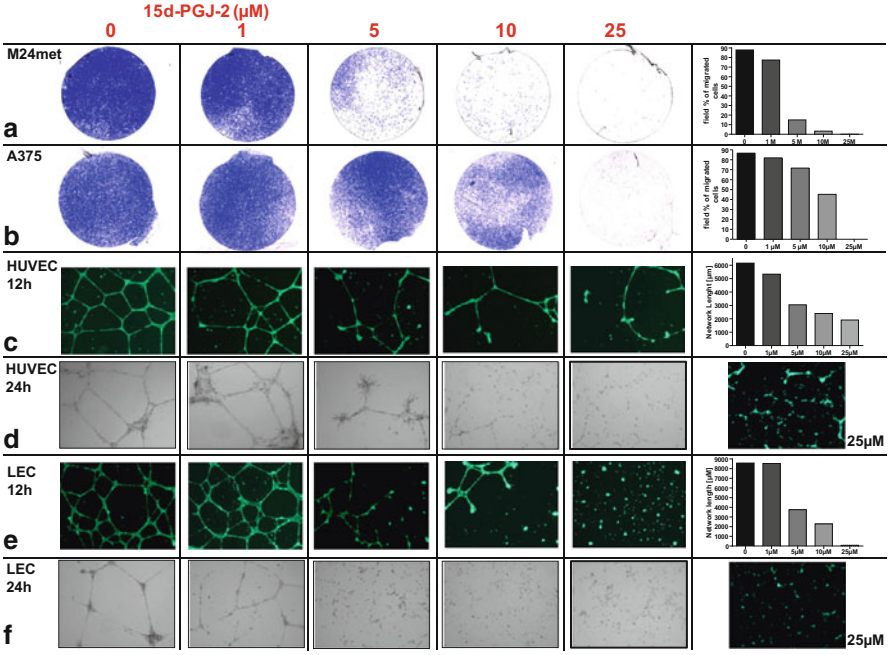

Fig. 8.3 15d-PGJ2 inhibits tumor cell migration and tube formation of HUVECs and LECs. **a** and **b** Tumor cell migration assay after 48 h of M24met melanoma cells and A375 melanoma cell line treated with 15d-PGJ2 with indicated concentrations. Representative pictures of three independent experiments. Quantification of the depicted experiment is performed using Axiovision Software. **c**–**f**, tube formation assay of HUVECs and LECs with indicated concentrations after 24 and 48 h. Calcein staining was performed to monitor the vitality of the cells. Tube formation was quantified using Cell Profiler Software Package. Representative pictures of three independent experiments

(Fig. 8.4c, Table 8.4) (Uniprot) were found to be downregulated. Evidence is growing that PPARγ ligands may be potent inhibitors of matrix metalloproteinases (MMPs) such as MMP 2, 7 and 9 [25–29]. The present shot gun proteomics data demonstrate downregulation of MMP 2, a key player in the metastatic process (Fig. 8.4c, Table 8.4). Employing a zymography assay we confirmed the downregulation of MMP2 by 15d-PGJ2 (Fig. 8.4d). To exclude unspecificity and cytotoxic side effects we evaluated if 15d-PGJ2 exhibits effects on the NF-kappa-B pathway. In the shotgun data we did not observe upregulation of constituents of the NF-kappa-B signalling pathway such as I-kappa-B-kinase 2 or NF-kappa-B inhibitor-interacting Ras-like protein 2 (Kappa B-Ras protein 2). In addition we observe no upregulation of NF-kappa-B by western blot analysis (data not shown).

Table 8.2 Upregulated candidates by 15d-PGJ2

Accession	Name	Number of Peptides	Score	Fractions	Function (Uniprot)
O00506	Serine/threonine-protein kinase 25	1	11.78	C	Oxidant stress-activated serine/threonine kinase that may play a role in the response to environmental stress. Targets to the Golgi apparatus where it appears to regulate protein transport events, cell adhesion, and polarity complexes important for cell migration. Phosphorylated upon DNA damage, probably by ATM or ATR
P11166	Solute carrier family 2, facilitated glucose transporter member 1	1	16.6	C	Facilitative glucose transporter. This isoform may be responsible for constitutive or basal glucose uptake. Transport. Phosphorylated upon DNA damage, probably by ATM or ATR
P02647	Apolipoprotein A-I (Apo-AI)	1	15.85	C	Participates in the reverse transport of cholesterol from tissues to the liver for excretion by promoting cholesterol efflux from tissues and by acting as a cofactor for the lecithin cholesterol acyltransferase (LCAT). Belongs to the apolipoprotein A1/A4/E family. Transport. Secreted
P61619	Protein transport protein Sec61 subunit alpha isoform 1	2	37.67	C, N	Plays a crucial role in the insertion of secretory and membrane polypeptides into the ER. Required for assembly of membrane and secretory proteins. Transport
O00203	AP-3 complex subunit beta-1	1	15.28	C	Subunit of non-clathrin- and clathrin-associated adaptor protein complex 3 that plays a role in protein sorting in the late-Golgi/trans-Golgi network (TGN) and/or endosomes. The AP complexes mediate both the recruitment of clathrin to membranes and the recognition of sorting signals within the cytosolic tails of transmembrane cargo molecules. AP-3 appears to be involved in the sorting of a subset of transmembrane proteins targeted to lysosomes and lysosome-related organelles. Protein Transport
O00400	Acetyl-coenzyme A transporter 1	1	17.26	C	Probable acetyl-CoA transporter necessary for O-acetylation of gangliosides. Transport
O43633	Charged multivesicular body protein 2a	1	18.49	C	Probable core component of the endosomal sorting required for transport complex III (ESCRT-III) which is involved in multivesicular bodies (MVBs) formation and sorting of endosomal cargo proteins into MVBs. MVBs are delivered to lysosomes enabling degradation of membrane proteins, such as stimulated growth factor receptors, lysosomal enzymes and lipids. Protein transport
O94979	Protein transport protein Sec31A	1	16.15	C	Component of the coat protein complex II (COPII) which promotes the formation of transport vesicles from the endoplasmic reticulum (ER). Protein transport

P03891	NADH-ubiquinone oxidoreductase chain 2	1	13.82	N	Core subunit of the mitochondrial membrane respiratory chain NADH dehydrogenase (Complex I) that is believed to belong to the minimal assembly required for catalysis. Complex I functions in the transfer of electrons from NADH to the respiratory chain. Transport
P07108	Acyl-CoA-binding protein (ACBP)	3	35.55	C	Binds medium- and long-chain acyl-CoA esters with very high affinity and may function as an intracellular carrier of acyl-CoA esters. It is also able to displace diazepam from the benzodiazepine (BZD) recognition site located on the GABA type A receptor. Transport
P08574	Cytochrome c1, heme protein, mitochondrial	1	14.1	N	This is the heme-containing component of the cytochrome b-c1 complex, which accepts electrons from Rieske protein and transfers electrons to cytochrome c in the mitochondrial respiratory chain. Transport
P21281	V-type proton ATPase subunit B, brain isoform	2	30.86	C	Non-catalytic subunit of the peripheral V1 complex of vacuolar ATPase. V-ATPase is responsible for acidifying a variety of intracellular compartments in eukaryotic cells. Identified by mass spectrometry in melanosome fractions from stage I to stage IV. Transport
P49755	Transmembrane emp24 domain-containing protein 10	1	13.61	C	Involved in vesicular protein trafficking. Identified by mass spectrometry in melanosome fractions from stage I to stage IV. Transport
P53985	Monocarboxylate transporter 1 (MCT 1)	1	13.46	C	Proton-linked monocarboxylate transporter. Transport. Widely expressed in normal and in cancer cells
P54709	Sodium/potassium-transporting ATPase subunit beta-3 (Sodium/potassium-dependent ATPase subunit beta-3) (ATPB-3)	1	14.44	C	This is the non-catalytic component of the active enzyme, which catalyzes the hydrolysis of ATP coupled with the exchange of Na+ and K+ ions across the plasma membrane. The exact function of the beta-3 subunit is not known. Identified by mass spectrometry in melanosome fractions from stage I to stage IV. Transport
P78363	Retinal-specific ATP-binding cassette transporter (ATP-binding cassette subfamily A member 4)	2	24.61	C	May play a role in photoresponse. Retinoids, and most likely retinal, are the natural substrates for transport by abcr in rod outer segments. Belongs to the ABC transporter superfamily. ABCA family. Transport
Q86UQ4	ATP-binding cassette sub-family A member 13	1	13.03	N	Transport

Table 8.2 (continued)

Accession	Name	Number of Peptides	Score	Fractions	Function (Uniprot)
Q96CW1	AP-2 complex subunit mu (Adapter-related protein complex 2 mu subunit) (Adaptor protein complex AP-2 subunit mu) (Adaptin-mu2) (AP-2 mu chain) (Plasma membrane adaptor AP-2 50 kDa protein) (HA2 50 kDa subunit) (Clathrin assembly protein complex 2 medium c	1	12.56	N	Component of the adaptor protein complex 2 (AP-2). Adaptor protein complexes function in protein transport via transport vesicles in different membrane traffic pathways. Adaptor protein complexes are vesicle coat components and appear to be involved in cargo selection and vesicle formation. AP-2 is involved in clathrin-dependent endocytosis in which cargo proteins are incorporated into vesicles surrrounded by clathrin (clathrin-coated vesicles, CCVs) which are destined for fusion with the early endosome
Q96M27	Protein PRRC1	1	15.1	C	Golgi apparatus
Q9UKS6	Protein kinase C and casein kinase substrate in neurons protein 3	1	13.92	N	May play a role in vesicle formation and transport
Q9Y5W7	Sorting nexin-14	1	14.65	C	May be involved in several stages of intracellular trafficking. Transport
O60231	Putative pre-mRNA-splicing factor ATP-dependent RNA helicase DHX16	1	17.61	N	Probable ATP-binding RNA helicase involved in pre-mRNA splicing
O60306	Intron-binding protein aquarius (Intron-binding protein of 160 kDa) (IBP160)	3	31.31	N	Intron-binding spliceosomal protein required to link pre-mRNA splicing and snoRNP (small nucleolar ribonucleoprotein) biogenesis
Q16560	U11/U12 small nuclear ribonucleoprotein 35 kDa protein	1	17.13	N	Component of the U11/U12 snRNPs that are part of the U12-type spliceosome
Q6PIY7	Poly(A) RNA polymerase GLD2 (hGLD-2) (PAP-associated domain-containing protein 4) (Terminal uridylyltransferase 2) (TUTase 2)	1	15.71	N	Cytoplasmic poly(A) RNA polymerase that adds successive AMP monomers to the 3′-end of specific RNAs, forming a poly(A) tail. In contrast to the canonical nuclear poly(A) RNA polymerase, it only adds poly(A) to selected cytoplasmic mRNAs. Does not play a role in replication-dependent histone mRNA degradation
Q96I25	Splicing factor 45 (45 kDa-splicing factor) (RNA-binding motif protein 17)	1	13.29	N	Splice factor that binds to the single stranded 3′AG at the exon/intron border and promotes its utilization in the second catalytic step. Involved in the regulation of alternative splicing and the utilization of cryptic splice sites. Promotes the utilization of a cryptic splice site created by the beta-110 mutation in the HBB gene. The resulting frameshift leads to sickle cell anemia

P63162	Small nuclear ribonucleoprotein-associated protein N	7	105.3	N	May be involved in tissue-specific alternative RNA processing events
Q12799	T-complex protein 10A homolog	1	11.85	C	Alternative Splicing
Q16637	Survival motor neuron protein (Component of gems 1) (Gemin-1)	1	13.83	C	The SMN complex plays an essential role in spliceosomal snRNP assembly in the cytoplasm and is required for pre-mRNA splicing in the nucleus. It may also play a role in the metabolism of snoRNPs
Q3KQU3	MAP7 domain-containing protein 1	1	15.84	C	Alternative Splicing
Q5T3F8	Transmembrane protein 63B	1	19.77	N	Membrane. Alternative Splicing
Q5T8P6	RNA-binding protein 26	1	16.07	N	Alternative Splicing
Q5TB30	DEP domain-containing protein 1A	1	12.2	C	Alternative Splicing. Up-regulated in bladder cancer cells (at protein level)
Q96D71	RalBP1-associated Eps domain-containing protein 1	1	13.78	C	May coordinate the cellular actions of activated EGF receptors and Ral-GTPases
Q14004	Cell division protein kinase 13 (Cell division cycle 2-like protein kinase 5) (CDC2-related protein kinase 5)	1	17.17	N	May be a controller of the mitotic cell cycle. Involved in the blood cell development. Also expressed in neuroblastoma and glioblastoma tumors. Phosphorylated upon DNA damage, probably by ATM or ATR
Q14839	Chromodomain-helicase-DNA-binding protein 4	1	12.43	N	Probable transcription regulator. Phosphorylated upon DNA damage, probably by ATM or ATR
Q99575	Ribonucleases P/MRP protein subunit POP1 (hPOP1)	2	29.55	N	Component of ribonuclease P, a protein complex that generates mature tRNA molecules by cleaving their 5′-ends. Also a component of RNase MRP Phosphorylated upon DNA damage, probably by ATM or ATR
Q9C0C2	182 kDa tankyrase-1-binding protein	4	54.84	C	Binds to the ANK repeat domain of TNKS1 and TNKS2. Phosphorylated upon DNA damage, probably by ATM or ATR
O60271	C-jun-amino-terminal kinase-interacting protein 4 (JNK-interacting protein 4)	1	16.37	C	The JNK-interacting protein (JIP) group of scaffold proteins selectively mediates JNK signaling by aggregating specific components of the MAPK cascade to form a functional JNK signaling module. Perinuclear distribution in response to stress signals such as UV radiation. Phosphorylated upon DNA damage, probably by ATM or ATR
P20585	DNA mismatch repair protein Msh3 (hMSH3) (Divergent upstream protein) (DUP) (Mismatch repair protein 1) (MRP1)	2	19.2	N	Component of the post-replicative DNA mismatch repair system (MMR). Heterodimerizes with MSH2 to form MutS beta which binds to DNA mismatches thereby initiating DNA repair. Phosphorylated upon DNA damage, probably by ATM or ATR

Table 8.2 (continued)

Accession	Name	Number of Peptides	Score	Fractions	Function (Uniprot)
Q02952	A-kinase anchor protein 12 (A-kinase anchor protein 250 kDa) (AKAP 250) (Gravin) (Myasthenia gravis autoantigen)	1	18.9	C	Anchoring protein that mediates the subcellular compartmentation of protein kinase A (PKA) and protein kinase C (PKC). Expressed in endothelial cells, cultured fibroblasts and osteosarcoma. Activated by lysophosphatidylcholine (lysoPC). Phosphorylated upon DNA damage, probably by ATM or ATR.
Q15554	Telomeric repeat-binding factor 2 (TTAGGG repeat-binding factor 2) (Telomeric DNA-binding protein)	1	14.27	N	Binds the telomeric double-stranded TTAGGG repeat. Protects against end-to-end fusion of chromosomes and plays a role in successful progression through the cell division cycle. Component of the shelterin complex (telosome) that is involved in the regulation of telomere length and protection. Phosphorylated upon DNA damage, probably by ATM or ATR. $ Shelterin associates with arrays of double-stranded TTAGGG repeats added by telomerase and protects chromosome ends; without its protective activity, telomeres are no longer hidden from the DNA damage surveillance and chromosome ends are inappropriately processed by DNA repair pathways
Q9H583	HEAT repeat-containing protein 1 (Protein BAP28)	3	36.74	N	Involved in nucleolar processing of pre-18S ribosomal RNA. Involved in ribosome biosynthesis Phosphorylated upon DNA damage, probably by ATM or ATR
Q9NPQ8	Synembryn-A (Protein Ric-8A)	2	29.98	C	Guanine nucleotide exchange factor (GEF), which can activate some, but not all, G-alpha proteins. Able to activate GNAI1, GNAO1 and GNAQ, but not GNAS by exchanging bound GDP for free GTP. Involved in regulation of microtubule pulling forces during mitotic movement of chromosomes by stimulating G(i)-alpha protein, possibly leading to release G(i)-alpha-GTP and NuMA proteins from the NuMA-GPSM2-G(i)-alpha-GDP complex By similarity. Also acts as an activator for G(q)-alpha (GNAQ) protein by enhancing the G(q)-coupled receptor-mediated ERK activation Phosphorylated upon DNA damage, probably by ATM or ATR
Q9UNF1	Melanoma-associated antigen D2 (MAGE-D2 antigen) (Breast cancer-associated gene 1 protein) (BCG-1) (11B6) (Hepatocellular carcinoma-associated protein JCL-1)	1	9.3	C	Phosphorylated upon DNA damage, probably by ATM or ATR

P24557	Thromboxane-A synthase (TXA synthase) (Cytochrome P450 5A1)	1	12.57	C	Belongs to the cytochrome P450 family. Fatty acid biosynthesis, Lipid synthesis, Prostaglandin biosynthesis
P30837	Aldehyde dehydrogenase X, mitochondrial (Aldehyde dehydrogenase family 1 member B1) (Aldehyde dehydrogenase 5)	1	12.33	C	ALDHs play a major role in the detoxification of alcohol-derived acetaldehyde. They are involved in the metabolism of corticosteroids, biogenic amines, neurotransmitters, and lipid peroxidation
P54619	5′-AMP-activated protein kinase subunit gamma-1 (AMPK subunit gamma-1)	1	21.4	C	AMPK is responsible for the regulation of fatty acid synthesis by phosphorylation of acetyl-CoA carboxylase. Also regulates cholesterol synthesis via phosphorylation and inactivation of hydroxymethylglutaryl-CoA reductase and hormone-sensitive lipase. Fatty acid biosynthesis, Lipid synthesis
Q14914	Prostaglandin reductase 1 (PRG-1) (NADP-dependent leukotriene B4 12-hydroxydehydrogenase) (15-oxoprostaglandin 13-reductase)	1	13.61	C	Functions as 15-oxo-prostaglandin 13-reductase and acts on 15-oxo-PGE1, 15-oxo-PGE2 and 15-oxo-PGE2-alpha. Has no activity towards PGE1, PGE2 and PGE2-alpha By similarity. Catalyzes the conversion of leukotriene B4 into its biologically less active metabolite, 12-oxo-leukotriene B4. This is an initial and key step of metabolic inactivation of leukotriene B4
Q96Q06	Perilipin-4 (Adipocyte protein S3-12)	1	16.51	C	May play a role in triacylglycerol packaging into adipocytes. May function as a coat protein involved in the biogenesis of lipid droplets Up-regulated during adipocyte differentiation
Q99541	Adipophilin (Adipose differentiation-related protein) (ADRP)	1	13.13	C	May be involved in development and maintenance of adipose tissue
P35659	Protein DEK	3	47.66	N	May have a function in the nucleus. DEK is found in a subset of acute myeloid leukemia (AML); also known as acute non-lymphocytic leukemia
P42695	Condensin-2 complex subunit D3 (Non-SMC condensin II complex subunit D3) (hCAP-D3)	1	12.79	N	Regulatory subunit of the condensin-2 complex, a complex which establishes mitotic chromosome architecture and is involved in physical rigidity of the chromatid axis. Cell cycle, cell division, mitosis
Q12974	Protein tyrosine phosphatase type IVA 2	1	17.79	C	Protein tyrosine phosphatase which stimulates progression from G1 into S phase during mitosis. Promotes tumors. Overexpressed in prostate tumor tissue

Table 8.2 (continued)

Accession	Name	Number of Peptides	Score	Fractions	Function (Uniprot)
Q15155	Nodal modulator 1 (pM5)	1	14.64	N	May antagonize Nodal signaling. Expressed in colon tumor tissue and in adjacent normal colonic mucosa. Pro-apoptotic, Anti-proliferation
Q15287	RNA-binding protein with serine-rich domain 1 (SR-related protein LDC2)	1	17.31	N	Component of a splicing-dependent multiprotein exon junction complex (EJC) deposited at splice junction on mRNAs
Q15477	Helicase SKI2W (Helicase-like protein) (HLP)	1	17.15	C	Helicase; has ATPase activity
Q16527	Cysteine and glycine-rich protein 2 (Cysteine-rich protein 2) (Smooth muscle cell LIM protein)	1	12.26	N	Drastically down-regulated in response to PDGF-BB or cell injury, that promote smooth muscle cell proliferation and dedifferentiation. Seems to play a role in the development of the embryonic vascular system
Q7KZ85	Transcription elongation factor SPT6 (hSPT6)	1	18.7	N	Acts to stimulate transcriptional elongation by RNA polymerase II
Q7L2E3	Putative ATP-dependent RNA helicase DHX30	2	24.85	N	no known function
Q7Z5K2	Wings apart-like protein homolog (Friend of EBNA2 protein)	1	14.39	N	May play a role in cell growth
Q8NBU5	ATPase family AAA domain-containing protein 1	1	17.16	N	Replication
Q8TF68	Zinc finger protein 384	1	13.86	N	Transcription factor that binds the consensus DNA sequence [GC]AAAAA. Seems to bind and regulate the promoters of MMP1, MMP3, MMP7 and COL1A1
Q969S3	Zinc finger protein 622 (Zinc fingerlike protein 9)	1	15.58	N	May behave as an activator of the bound transcription factor, MYBL2, and be involved in embryonic development
Q96RK0	Protein capicua homolog	1	12.71	C	Transcriptional repressor which may play a role in development of the central nervous system (CNS)
Q9H6F5	Coiled-coil domain-containing protein	1	14.65	N	Nuclear
Q9Y5V0	Zinc finger protein 706	1	13.22	N	Zinc finger protein
O00754	Lysosomal alpha-mannosidase (Laman)	1	14.91	C	Necessary for the catabolism of N-linked carbohydrates released during glycoprotein turnover. Cleaves all known types of alpha-mannosidic linkages

O14880	Microsomal glutathione S-transferase 3	1	15.48	N	Functions as a glutathione peroxidase
O15143	Actin-related protein 2/3 complex subunit 1B (Arp2/3 complex 41 kDa subunit) (p41-ARC)	1	15.84	C	Functions as component of the Arp2/3 complex which is involved in regulation of actin polymerization and together with an activating nucleation-promoting factor (NPF) mediates the formation of branched actin networks
O15511	Actin-related protein 2/3 complex subunit 5 (Arp2/3 complex 16 kDa subunit) (p16-ARC)	1	13.18	C	Functions as component of the Arp2/3 complex which is involved in regulation of actin polymerization and together with an activating nucleation-promoting factor (NPF) mediates the formation of branched actin networks
O43516	WAS/WASL-interacting protein family member 1	1	12.63	C	May have direct activity on the actin cytoskeleton. Induces actin polymerization and redistribution
O75179	Ankyrin repeat domain-containing protein 17	1	15.62	C	Earliest specific in situ marker of hepatic differentiation during embryogenesis, useful for characterization of inductive events involved in hepatic specification
O75293	Growth arrest and DNA damage-inducible protein GADD45 beta	1	11.3	C	Involved in the regulation of growth and apoptosis. Mediates activation of stress-responsive MTK1/MEKK4 MAPKKK
O76039	Cyclin-dependent kinase-like 5 (Serine/threonine-protein kinase 9)	1	12.29	N	Mediates phosphorylation of MECP2
O94804	Serine/threonine-protein kinase 10 (Lymphocyte-oriented kinase)	1	14.73	C	Can act on substrates such as myelin basic protein and histone 2A on serine and threonine residues
O95139	NADH dehydrogenase [ubiquinone] 1 beta subcomplex subunit 6 (NADH-ubiquinone oxidoreductase B17 subunit) (Complex I-B17) (CI-B17)	1	12.64	N	Accessory subunit of the mitochondrial membrane respiratory chain NADH dehydrogenase (Complex I), that is believed not to be involved in catalysis. Complex I functions in the transfer of electrons from NADH to the respiratory chain. The immediate electron acceptor for the enzyme is believed to be ubiquinone
P05362	Intercellular adhesion molecule 1 (ICAM-1) (Major group rhinovirus receptor)	1	12.01	C	ICAM proteins are ligands for the leukocyte adhesion protein LFA-1 (integrin alpha-L/beta-2). During leukocyte transendothelial migration, ICAM1 engagement promotes the assembly of endothelial apical cups through SGEF and RHOG activation
P09601	Heme oxygenase 1 (HO-1)	2	19.3	C	Heme oxygenase cleaves the heme ring at the alpha methene bridge to form biliverdin. Biliverdin is subsequently converted to bilirubin by biliverdin reductase

Table 8.2 (continued)

Accession	Name	Number of Peptides	Score	Fractions	Function (Uniprot)
P10636	Microtubule-associated protein tau (Neurofibrillary tangle protein) (Paired helical filament-tau) (PHF-tau)	1	13.28	N	Promotes microtubule assembly and stability, and might be involved in the establishment and maintenance of neuronal polarity. The C-terminus binds axonal microtubules while the N-terminus binds neural plasma membrane components, suggesting that tau functions as a linker protein between both
P11279	Lysosome-associated membrane glycoprotein 1 (LAMP-1) (CD107 antigen-like family member A)	1	15.01	C	Presents carbohydrate ligands to selectins. Also implicated in tumor cell metastasis
P11474	Steroid hormone receptor ERR1 (Estrogen-related receptor alpha) (ERR-alpha) (Estrogen receptor-like 1) (Nuclear receptor subfamily 3 group B member 1)	1	13.81	N	Belongs to the nuclear hormone receptor family. Binds to an ERR-alpha response element (ERRE) containing a single consensus half-site. Binds DNA as a monomer or a homodimer
P16615	Sarcoplasmic/endoplasmic reticulum calcium ATPase 2	3	44.84	C, N	This magnesium-dependent enzyme catalyzes the hydrolysis of ATP coupled with the translocation of calcium from the cytosol to the sarcoplasmic reticulum lumen
P16930	Fumarylacetoacetase (FAA)	1	12.36	C	4-fumarylacetoacetate $+H_2O =$ acetoacetate + fumarate
P17275	Transcription factor jun-B	1	12.94	N	Transcription factor involved in regulating gene activity following the primary growth factor response. Binds to the DNA sequence 5′-TGA[CG]TCA-3′. Transcription
P17661	Desmin	1	12.85	N	Desmin are class-III intermediate filaments found in muscle cells. Belongs to the intermediate filament family
P27105	Erythrocyte band 7 integral membrane protein (Stomatin)	2	27.52	C, N	Thought to regulate cation conductance. Identified by mass spectrometry in melanosome fractions
P29144	Tripeptidyl-peptidase 2	1	13.67	C	Component of the proteolytic cascade acting downstream of the 26S proteasome in the ubiquitin-proteasome pathway
P30043	Flavin reductase (FR) (NADPH-dependent diaphorase)	1	15.75	C	Broad specificity oxidoreductase that catalyzes the NADPH-dependent reduction of a variety of flavins, such as riboflavin, FAD or FMN, biliverdins, methemoglobin and PQQ (pyrroloquinoline quinone). Contributes to heme catabolism and metabolizes linear tetrapyrroles

P35613	Basigin (Leukocyte activation antigen M6) (Collagenase stimulatory factor)	2	26.82	C	Plays pivotal roles in spermatogenesis, embryo implantation, neural network formation and tumor progression. Stimulates adjacent fibroblasts to produce matrix metalloproteinases (MMPS). Seems to be a receptor for oligomannosidic glycans. In vitro, promotes outgrowth of astrocytic processes. Enriched on the surface of tumor cells. Up-regulated in gliomas. Its expression levels correlate with malignant potential of the tumor
P36957	Dihydrolipoyllysine-residue succinyltransferase component of 2-oxoglutarate dehydrogenase complex, mitochondrial	1	19.07	N	The 2-oxoglutarate dehydrogenase complex catalyzes the overall conversion of 2-oxoglutarate to succinyl-CoA and CO_2. It contains multiple copies of 3 enzymatic components: 2-oxoglutarate dehydrogenase (E1), dihydrolipoamide succinyltransferase (E2) and lipoamide dehydrogenase (E3). Mitochondrial
P40121	Macrophage-capping protein (Actin regulatory protein CAP-G)	1	12.89	C	Calcium-sensitive protein which reversibly blocks the barbed ends of actin filaments but does not sever preformed actin filaments. May play an important role in macrophage function. May play a role in regulating cytoplasmic and/or nuclear structures through potential interactions with actin. May bind DNA. Identified by mass spectrometry in melanosome fractions from stage I to stage IV
P48163	NADP-dependent malic enzyme (NADP-ME) (Malic enzyme 1)	1	14.28	C	(S)-malate + NADP+ = pyruvate + CO_2 + NADPH. Oxidoreductase
P49662	Caspase-4 (CASP-4) (Protease ICH-2) (Protease TX) (ICE(rel)-II)	1	13.83	C	Involved in the activation cascade of caspases responsible for apoptosis execution. Cleaves caspase-1
P55786	Puromycin-sensitive aminopeptidase (PSA)	4	52.95	C	Aminopeptidase with broad substrate specificity to several peptides. Involved in proteolytic events essential for cell growth and viability. Identified by mass spectrometry in melanosome fractions from stage I to stage IV
P57088	Transmembrane protein 33 (Protein DB83)	1	17.38	C, N	Transmembrane. Identified by mass spectrometry in melanosome fractions from stage I to stage IV
Q14139	Ubiquitin conjugation factor E4 A	1	11.97	C	Binds to the ubiquitin moieties of preformed conjugates and catalyzes ubiquitin chain assembly in conjunction with E1, E2, and E3. mRNA processing
Q14147	Probable ATP-dependent RNA helicase DHX34	1	12.57	N	Probable ATP-binding RNA helicase
Q15819	Ubiquitin-conjugating enzyme E2 variant 2 (MMS2) (Enterocyte	2	24.62	C	Has no ubiquitin ligase activity on its own. The UBE2V2/UBE2N heterodimer catalyzes the synthesis of non-canonical poly-ubiquitin

Table 8.2 (continued)

Accession	Name	Number of Peptides	Score	Fractions	Function (Uniprot)
	differentiation-associated factor EDAF-1) (Enterocyte differentiation-promoting factor) (EDPF-1) (Vitamin D3-inducible protein) (DDVit 1)				chains that are linked through 'Lys-63'. This type of poly-ubiquitination does not lead to protein degradation by the proteasome. Mediates transcriptional activation of target genes. Plays a role in the control of progress through the cell cycle and differentiation. Plays a role in the error-free DNA repair pathway and contributes to the survival of cells after DNA damage
Q16719	Kynureninase	3	40.75	C	Pyridine nucleotide biosynthesis
Q5T655	Coiled-coil domain-containing protein	1	14.65	C	Not known
Q6WCQ1	Myosin phosphatase Rho-interacting protein (M-RIP) (Rho-interacting protein 3) (RIP3) (p116Rip)	1	14.68	N	Targets myosin phosphatase to the actin cytoskeleton. Required for the regulation of the actin cytoskeleton by RhoA and ROCK1. Depletion leads to an increased number of stress fibers in smooth muscle cells through stabilization of actin fibers by phosphorylated myosin. Overexpression of MRIP as well as its F-actin-binding region leads to disassembly of stress fibers in neuronal cells
Q6ZS46	Putative uncharacterized protein FLJ45840	1	12.15	N	no known function
Q7Z2T5	TRM1-like protein	1	13.84	N	May play a role in motor coordination and exploratory behavior
Q7Z6I8	UPF0461 protein C5orf24	1	13.57	N	no known function
Q8IW41	MAP kinase-activated protein kinase 5	1	14.63	C	Mediates stress-induced small heat shock protein 27 phosphorylation
Q8IY37	Probable ATP-dependent RNA helicase DHX37 (DEAH box protein 37)	2	29.56	N	Belongs to the DEAD box helicase family. DEAH subfamily
Q8N6L1	Keratinocyte-associated protein 2 (KCP-2)	1	13.2	N	Component of the oligosaccharyltransferase (OST) complex. OST seems to exist in different forms which contain at least RPN1, RPN2, OST48, DAD1, OSTC, KRTCAP2 and either STT3A or STT3B. OST can form stable complexes with the Sec61 complex or with both the Sec61 and TRAP complexes
Q8N766	Uncharacterized protein KIAA0090	1	13.36	N	no known function
Q8NA47	Coiled-coil domain-containing protein	1	13.18	N	no known function
Q8NEF9	Serum response factor-binding protein 1 (SRF-dependent transcription regulation-associated protein) (p49/STRAP)	1	13.53	N	May be involved in regulating transcriptional activation of cardiac genes during the aging process. May play a role in biosynthesis and/or processing of SLC2A4 in adipose cells

Q8TBC4	NEDD8-activating enzyme E1 catalytic subunit (Ubiquitin-like modifier-activating enzyme 3) (Ubiquitin-activating enzyme 3) (NEDD8-activating enzyme E1C) (Ubiquitin-activating enzyme E1C)	1	14.4	C	Catalytic subunit of the dimeric UBA3-NAE1 E1 enzyme. E1 activates NEDD8 by first adenylating its C-terminal glycine residue with ATP, thereafter linking this residue to the side chain of the catalytic cysteine, yielding a NEDD8-UBA3 thioester and free AMP. E1 finally transfers NEDD8 to the catalytic cysteine of UBE2M. Down-regulates steroid receptor activity. Necessary for cell cycle progression
Q96KB5	Lymphokine-activated killer T-cell-originated protein kinase	1	14.29	C	Phosphorylates MAP kinase p38. Seems to be active only in mitosis. May also play a role in the activation of lymphoid cells. When phosphorylated, forms a complex with TP53, leading to TP53 destabilization and attenuation of G2/M checkpoint during doxorubicin-induced DNA damage
Q96N11	Uncharacterized protein C7orf26	1	11.54	N	No known function
Q9BQ52	Zinc phosphodiesterase ELAC protein 2	1	13.44	C	Zinc phosphodiesterase, which displays some tRNA 3′-processing endonuclease activity. Probably involved in tRNA maturation, by removing a 3′-trailer from precursor tRNA
Q9BV86	Methyltransferase-like protein 11A	1	12.02	C	Probable S-adenosyl-L-methionine-dependent methyltransferase
Q9BZ29	Dedicator of cytokinesis protein 9 (Cdc42 guanine nucleotide exchange factor zizimin-1)	1	12.47	C	Guanine nucleotide-exchange factor (GEF) that activates CDC42 by exchanging bound GDP for free GTP. Overexpression induces filopodia formation
Q9GZS1	DNA-directed RNA polymerase I subunit RPA49 (RNA polymerase I subunit A49) (DNA-directed RNA polymerase I subunit E) (RNA polymerase I-associated factor 1) (RNA polymerase I-associated factor 53)	1	12.69	N	DNA-dependent RNA polymerase catalyzes the transcription of DNA into RNA using the four ribonucleoside triphosphates as substrates. Component of RNA polymerase I which synthesizes ribosomal RNA precursors. Appears to be involved in the formation of the initiation complex at the promoter by mediating the interaction between Pol I and UBTF/UBF
Q9H501	ESF1 homolog (ABT1-associated protein)	1	12.72	N	May constitute a novel regulatory system for basal transcription. Negatively regulates ABT1
Q9H853	Putative tubulin-like protein alpha-4B (Alpha-tubulin 4B)	2	23.58	N	cytoskeleton
Q9NSD9	Phenylalanyl-tRNA synthetase beta chain (Phenylalanine–tRNA ligase beta chain) (PheRS)	3	44.85	N	ATM target
Q9NUQ9	Protein FAM49B (L1)	1	13.07	C	No known function
Q9NX40	OCIA domain-containing protein 1	3	41.16	C, N	No known function

Table 8.2 (continued)

Accession	Name	Number of Peptides	Score	Fractions	Function (Uniprot)
Q9NZA1	Chloride intracellular channel protein 5	1	13	C	Can insert into membranes and form poorly selective ion channels that may also transport chloride ions. May play a role in the regulation of transepithelial ion absorption and secretion. Required for normal formation of stereocilia in the inner ear and normal development of the organ of Corti
Q9P000	COMM domain-containing protein 9	1	16.62	C	No known function
Q9P2D3	HEAT repeat-containing protein 5B	1	15.1	C	No known function
Q9UET6	Putative ribosomal RNA methyltransferase 1	1	14.55	C	S-adenosyl-L-methionine + rRNA = S-adenosyl-L-homocysteine + rRNA containing 2′-O-methyluridine.
Q9UJY1	Heat shock protein beta-8 (HspB8)	1	13.43	C	Displays temperature-dependent chaperone activity
Q9UM00	Transmembrane and coiled-coil domain-containing protein 1	1	13.21	N	Endoplasmic reticulum membrane;
Q9UM54	Myosin-VI (Unconventional myosinVI)	2	26.36	C	Transport
Q9Y263	Phospholipase A-2-activating protein (PLA2P)	1	15.17	C	Plays an important role in the regulation of specific inflammatory disease processes
Q9Y2R0	Coiled-coil domain-containing protein	1	14.32	C	No known function
Q9Y399	28S ribosomal protein S2, mitochondrial (S2mt)	1	14.43	C	Component of the mitochondrial ribosome small subunit (28S)
Q9Y5T4	DnaJ homolog subfamily C member 15 (Methylation-controlled J protein) (MCJ) (Cell growth-inhibiting gene 22 protein)	1	17	N	Absent or down-regulated in many advanced cases of ovarian adenocarcinoma, due to hypermethylation and allelic loss. Loss expression correlates with increased resistance to antineoplastic drugs, such as cisplatin

Proteins induced by 5 μM 15d-PGJ2 in A375 melanoma cells after 48 h. The proteins are classified by the CPL/MUW database. Uniprot serves as reference for the function of the proteins. In addition, the accession numbers are from the Uniprot database. Numbers indicate distinct peptides identified by mass spectrometry. C: cytoplasm, N: nucleous, S: supernatant

Table 8.3 Categories of upregulated candidates by 15d-PGJ2

Accession	Transport	mRNA processing	ATM target	Lipid metabolism	Nuclear	cell cycle	Cell Stress	Ciplatin-R	Cytoskeleton	Detoxification	DNA damage/repair	Drug resistance	ECM	Genuinely Secreted	Inflammation	Lysosome	Membrane	Migration	Mitochondrial	Pro-apoptotic	Proteases/Inhibitors	Protein degradation	Protein synthesis	Redox	Replication	Ribosomal	signalling	Transcription	Activation	Anti-apoptotic
O00506	x		x				x											x									x			
P11166	x		x																											
P02647	x			x										x																
P61619	x				x			x																						
O00203	x															x														
O00400	x																													
O43633	x															x														
O94979	x																													
P03891	x																		x											
P07108	x																													
P08574	x							x											x											
P21281	x																													
P49755	x																x													
P53985	x																													
P54709	x																													
P78363	x									x																				
Q86UQ4	x																													
Q96CW1	x																													
Q96M27	x																													
Q9UKS6	x																												x	
Q9Y5W7	x																													
O60231		x			x																									
O60306		x			x																									
Q16560		x			x																									
Q6PIY7		x			x																									
Q96I25		x			x																									
P63162		x																												
Q12799		x																												
Q16637		x																												
Q3KQU3		x																												
Q5T3F8		x															x													
Q5T8P6		x																												
Q5TB30		x																												
Q96D71		x																												
Q14004			x		x	x		x			x																x			
Q14839			x		x																						x			
Q99575			x		x																									
Q9C0C2			x		x																									
O60271			x																										x	
P20585			x								x																			

Table 8.3 (continued)

Accession	Transport	mRNA processing	ATM target	Lipid metabolism	Nuclear	cell cycle	Cell Stress	Ciplatin-R	Cytoskeleton	Detoxification	DNA damage/repair	Drug resistance	ECM	Genuinely Secreted	Inflammation	Lysosome	Membrane	Migration	Mitochondrial	Pro-apoptotic	Proteases/Inhibitors	Protein degradation	Protein synthesis	Redox	Replication	Rhibosomal	signalling	Transcription	Activation	Anti-apoptotic
Q02952			x																											
Q15554			x								x														x					
Q9H583			x																				x							
Q9NPQ8			x																											
Q9UNF1			x																											
P24557				x						x																				
P30837				x															x											
P54619				x																										
Q14914				x																										
Q96Q06				x																										
Q99541				x																										
P35659					x			x																						
P42695					x	x																			x					
Q12974					x	x																			x					
Q15155					x															x										
Q15287					x																									
Q15477					x																									
Q16527					x																									
Q7KZ85					x																						x			
Q7L2E3					x																									
Q7Z5K2					x																									
Q8NBU5					x																				x					
Q8TF68					x																						x			
Q969S3					x																						x			
Q96RK0					x																									
Q9H6F5					x																									
Q9Y5V0					x																									
O00754														x		x														
O14880										x														x						
O15143									x									x												
O15511								x	x									x												
O43516									x																					
O75293											x									x					x				x	
O76039																									x					
O94804																											x			
O95139																			x											
P05362								x						x	x			x												
P09601																													x	
P10636									x																					
P11279														x		x	x	x												
P11474																													x	
P17275																									x			x		
P17661									x																					
P27105												x																		
P29144																						x								
P30043																								x						

Table 8.3 (continued)

Accession	Transport	mRNA processing	ATM target	Lipid metabolism	Nuclear	cell cycle	Cell Stress	Ciplatin-R	Cytoskeleton	Detoxification	DNA damage/repair	Drug resistance	ECM	Genuinely Secreted	Inflammation	Lysosome	Membrane	Migration	Mitochondrial	Pro-apoptotic	Proteases/Inhibitors	Protein degradation	Protein synthesis	Redox	Replication	Ribosomal	signalling	Transcription	Activation	Anti-apoptotic
P35613													x	x				x			x									
P36957																			x											
P40121								x	x																					
P48163																								x						
P49662																				x										
P55786																									x					
P57088																	x													
Q14139																						x								
Q15819							x					x										x								
Q16719																							x							
Q6WCQ1									x									x												
Q8IW41								x																					x	x
Q8IYD1									x														x							
Q8NEF9																												x		
Q8TBC4																									x					
Q96KB5								x																						
Q9BQ52																							x							
Q9BZ29																		x												
Q9GZS1																									x					
Q9H501																												x		
Q9H853									x																					
Q9NSD9								x															x							
Q9UET6																										x				
Q9UJY1							x																							
Q9Y263															x															
Q9Y399																			x							x				

Proteins induced by 5 μM 15d-PGJ2 in A375 melanoma cells after 48 h. The proteins are classified by the CPL/MUW database. Uniprot serves as reference
for the function of the proteins. In addition, the accession numbers are from the Uniprot database. Numbers indicate distinct peptides identified by mass
spectrometry. C: cytoplasm, N: nucleous, S: supernatant

15d-PGJ2 Highly Downregulates a Panel of Chaperones and Leads to a Modification of Hsp90 in 2D-gel Electrophoresis

A large group of 33 out of 38 detectable chaperones were downregulated (Table 8.5). Especially Hsp90 beta (− 15) and alpha (− 13) revealed to be the most prominent downregulated chaperones upon 15d-PGJ2 treatment (Table 8.5). However, Western blotting of the cytoplasmic fractions and total cell lysates of A375 and 1205Lu cells did not verify these results (Fig. 8.6a, b). Using the total cell lysate again no regulation of Hsp90 could be verified in A375 and 1205Lu melanoma cell lines, only an induction of the additional appearing band of Hsp56 (Fig. 8.6b).

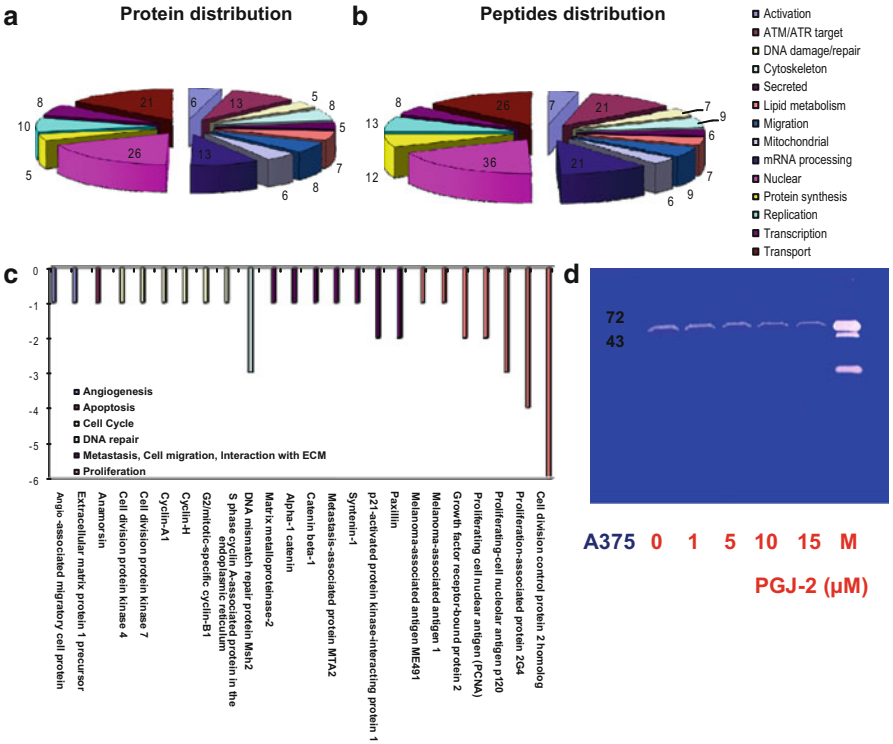

Fig. 8.4 Shot gun analysis and Zymography of A375 melanoma cells treated with 15d-PGJ2. **a** and **b** classification of all induced proteins and peptides by the bioinformatic database of A375 melanoma cells treated with 5 μM 15d-PGJ2 for 48 h. **c** downregulated proteins by 5 μM 15d-PGJ2 identified by shot gun analysis. The legend depicts the classification of the identified proteins. **d** Zymography assay of the supernatant of A375 melanoma cells treated with 1, 5, 10, 15 μM 15d-PGJ2 for 48 h

To further investigate these surprising results we performed 2D-gel electrophoresis with cytoplasmic proteins of A375 melanoma cells. Intriguingly, Hsp90 displayed a profound pI shift from 5.2–5.4 in the control group to 5.0–5.2 upon 15d-PGJ2 treatment (Fig. 8.6c). This indicates posttranslational modifications of Hsp90 which may cause interference with the identification of peptides by shot gun analysis. This shift is visualized also in a 3 dimensional version of the 2D-gel (Fig. 8.6c).

Protein modification may result in apparent down-regulation of the number of identified peptides, because modified peptides may fail to be identified by mass spectrometry. Therefore, we further investigated protein phosphorylation by immunoprecipitation using an anti-phosphoserine antibody. Actually, all chaperones identified in the immunoprecipitates were found at increased levels in the 15d-PGJ2 treated samples (Hsp90, Hsp27,T-complex protein 1 subunit theta and eta), indicating 15d-PGJ2-induced phosphorylation (Fig. 8.6d). These chaperones were found to be apparently down-regulated by 15d-PGJ2 (Table 8.5), suggesting that partially the down-regulation observed by shotgun proteomics is accompanied by phosphorylation.

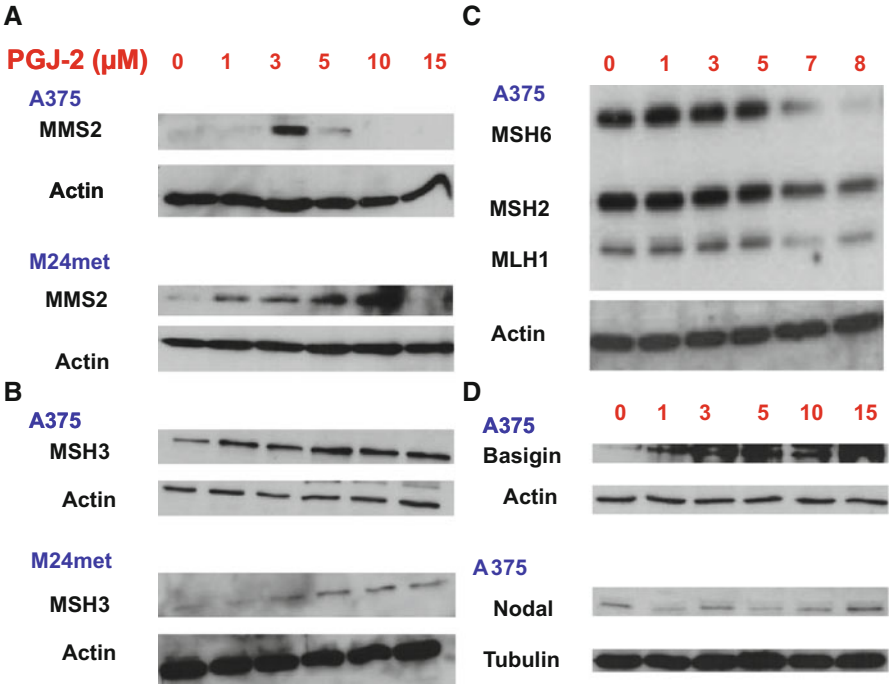

Fig. 8.5 Representative immunoblots of three independent experiments of MMS2, MSH3, MSH6, MSH2, MLH1, Basigin and nodal after 48 h treatment of 15d-PGJ2 with indicated concentrations (all concentrations are in μM)

Discussion

This study was designed to investigate consequences of PPARγ activation for melanoma and melanoma-associated stroma cells. While recent reports indicate antiproliferative effects of these drugs in several cancer cells including melanoma, this is the first investigation of PPARγ ligand effects including both melanoma cells as well as melanoma-associated stroma cells such as fibroblasts and endothelial cells.

We demonstrated that 15d-PGJ2 is much more effective compared to other PPARγ ligands in inhibiting growth of melanoma cell lines, while the PPARα ligand WY-14643 had hardly any effect. These results are in line with recent data of other laboratories [3]. Therefore we restricted subsequent analyses to 15d-PGJ2.

Prakash et al. demonstrated that 15d-PGJ2 induces cell death in B16F10 melanoma and addition of serum leads to a tolerance to 15d-PGJ2 by rapidly binding to albumin [30].

Our results support previous reports of PPARγ agonists describing both a direct anti-tumor and a broad spectrum of anti-stromal, anti-angiogenetic and immuno-modulating activities [29].

Table 8.4 Downregulated candidates by 15d-PGJ2

AccNr	Name	Control	15d-PGJ2 (5 μM)	Function (Ref. Uniprot)
Q13685	Angio-associated migratory cell protein	1	0	Plays a role in angiogenesis and cell migration
Q16610	Extracellular matrix protein 1 precursor	1	0	Involved in endochondral bone formation as negative regulator of bone mineralization. Stimulates the proliferation of endothelial cells and promotes angiogenesis
Q6FI81	Anamorsin	1	0	May be required for the maturation of extramitochondrial Fe/S proteins. Has anti-apoptotic effects in the cell
P11802	Cell division protein kinase 4	1	0	Probably involved in the control of the cell cycle. Defects in CDK4 are a cause of susceptibility to cutaneous malignant melanoma type 3 (CMM3)
P50613	Cell division protein kinase 7	1	0	Cyclin-dependent kinases (CDKs) are activated by the binding to a cyclin and mediate the progression through the cell cycle
P78396	Cyclin-A1	1	0	May be involved in the control of the cell cycle at the G1/S (start) and G2/M (mitosis) transitions
P51946	Cyclin-H	1	0	Regulates CDK7, the catalytic subunit of the CDK-activating kinase (CAK) enzymatic complex. Involved in cell cycle control
P14635	G2/mitotic-specific cyclin-B1	1	0	Essential for the control of the cell cycle at the G2/M (mitosis) transition
Q9BY12	S phase cyclin A-associated protein in the endoplasmic reticulum	1	0	CCNA2/CDK2 regulatory protein that transiently maintains CCNA2 in the cytoplasm
P43246	DNA mismatch repair protein Msh2	4	1	Component of the post-replicative DNA mismatch repair system (MMR). Forms two different heterodimers: MutS alpha (MSH2-MSH6 heterodimer) and MutS beta (MSH2-MSH3 heterodimer) which binds to DNA mismatches thereby initiating DNA repair
P08253	Matrix metallopro-teinase-2	1	0	Ubiquitinous metalloproteinase that is involved in diverse functions such as remodeling of the vasculature, angiogenesis, tissue repair, tumor invasion, inflammation, and atherosclerotic plaque rupture

P35221	Alpha-1 catenin	2	1	Associates with the cytoplasmic domain of a variety of cadherins. The association of catenins to cadherins produces a complex which is linked to the actin filament network, and which seems to be of primary importance for cadherins cell-adhesion properties. Can associate with both E- and N-cadherins. May play a crucial role in cell differentiation
P35222	Catenin beta-1	1	0	Involved in the regulation of cell adhesion. The majority of beta-catenin is localized to the cell membrane and is part of E-cadherin/catenin adhesion complexes which are proposed to couple cadherins to the actin cytoskeleton [32]
O94776	Metastasis-associated protein MTA2	1	0	May be involved in the regulation of gene expression as repressor and activator. The repression might be related to covalent modification of histone proteins
O00560	Syntenin-1	1	0	Seems to function as an adapter protein. In adherens junctions may function to couple syndecans to cytoskeletal proteins or signaling components. Seems to couple transcription factor SOX4 to the IL-5 receptor (IL5RA). May also play a role in vesicular trafficking. Seems to be required for the targeting of TGFA to the cell surface in the early secretory pathway
Q9NWT1	p21-activated protein kinase-interacting protein 1	3	1	Negatively regulates the PAK1 kinase. PAK1 is a member of the PAK kinase family, which have been shown to play a positive role in the regulation of signaling pathways involving MAPK8 and RELA
P49023	Paxillin	2	0	Cytoskeletal protein involved in actin-membrane attachment at sites of cell adhesion to the extracellular matrix (focal adhesion)
P08962	Melanoma-associated antigen ME491	1	0	This antigen is associated with early stages of melanoma tumor progression. May play a role in growth regulation
P43355	Melanoma-associated antigen 1	1	0	Not known, though may play a role in embryonal development and tumor transformation or aspects of tumor progression. Antigen recognized on a melanoma by autologous cytolytic T-lymphocytes

Table 8.4 (continued)

AccNr	Name	Control	15d-PGJ2 (5 μM)	Function (Ref. Uniprot)
P62993	Growth factor receptor-bound protein 2	2	0	Adapter protein that provides a critical link between cell surface growth factor receptors and the Ras signaling pathway
P12004	Proliferating cell nuclear antigen (PCNA)	6	4	This protein is an auxiliary protein of DNA polymerase delta and is involved in the control of eukaryotic DNA replication by increasing the polymerase's processibility during elongation of the leading strand
P46087	Proliferating-cell nucleolar antigen p120	6	3	May play a role in the regulation of the cell cycle and the increased nucleolar activity that is associated with the cell proliferation
Q9UQ80	Proliferation-associated protein 2G4	13	9	May play a role in a ERBB3-regulated signal transduction pathway. Seems be involved in growth regulation
P06493	Cell division control protein 2 homolog	6	0	Plays a key role in the control of the eukaryotic cell cycle. It is required in higher cells for entry into S-phase and mitosis

Proteins downregulated by 5 μM 15d-PGJ2 in A375 melanoma cells after 48 h. Uniprot serves as reference for the function of the proteins. In addition, the accession numbers are from the Uniprot database. Numbers indicate distinct peptides identified by mass spectrometry

Analysis of 15d-PGJ2 effects on melanoma-associated fibroblasts revealed substantial anti-proliferative effects. This finding points to a distinct effect of 15d-PGJ2 on cells in the tumor microenvironment, as normal fibroblasts did not show such a drug response.

Besides fibroblasts, endothelial cells are important players in the tumor microenvironment. Here we demonstrate that 15d-PGJ2 effectively abolished tube formation of HUVECs, which is in line with the observations that HUVEC differentiation into tube-like structures in three-dimensional collagen gels could be suppressed by specific PPARγ ligands [31]. Another anti-angiogenic mechanism is the induction of apoptotic cell death in endothelial cells after incubation with 15d-PGJ2 [32, 33]. In contrast to these data, we observed a rather high IC50 of HUVECs for 15d-PGJ2, suggesting that 15d-PGJ2 specifically interferes with the tube formation process. Since tube formation was inhibited already at a concentration of 5 μM and the cells were demonstrate to be still vital with the highest concentration tested, while the IC50 was found to be 85 μM, the destruction of the HUVEC tube formation is apparently not a result of growth inhibitory effects of 15d-PGJ2. This interpretation is supported by the finding that15d-PGJ2 transiently inhibits the expression of VEGFR-1 and VEGFR-2 [34].

The effect of 15d-PGJ2 on lymphatic endothelial cells has not been analyzed so far. In this study we provide evidence that 15d-PGJ2 also exerts anti-lymphangiogenic activity. The ability to promote lymphangiogenesis enhances the metastatic spread of melanoma and recent studies revealed that tumor associated lymphangiogenesis is significantly correlated with poor disease-free and overall survival of patients with cutaneous melanoma [35, 36]. The mechanism how, 15d-PGJ2 leads to an inhibition of lymphangiogensis has to be elucidated in further studies, since this activity adds to its potential as a therapeutic tool.

Tumor initiation and progression is associated with the transition of normal stroma into an "activated" stroma phenotype. These tumor-associated, genetically still intact cells are able to establish a supportive environment for tumor cell survival and growth and to facilitate invasion and metastasis. Targeting this interference between tumor and stroma may consistently lead to a reduction of tumor growth and metastasis. Such a therapeutic approach has been presented as biomodulatory treatment both by our group and others [37, 38] and may complement standard chemotherapeutic approaches.

In search for alternative strategies for the treatment of metastatic neoplasm, targeting the tumor stroma seems to be a promising strategy since this approach is not directly cytotoxic but interferes with the cooperativity of tumor and stroma cells [37–39]. Considering that the stroma provides proteins supporting tumor survival, a blockage of this process might chemosensitize the tumor cells. Here we showed for the first time that the receptor is expressed on a panel of melanoma associated fibroblasts while to a lower extent on normal fibroblasts such as TF. PPARγ expression in metastatic melanoma was shown to be a possible predictive marker for response to biomodulatory stroma-targeted therapy, since patients with PPARγ-positive metastases showed a significantly prolonged progression-free survival treated with biomodulatory treatment [38]. The expression of PPARγ protein

Table 8.5 Regulated chaperones and Heat shock proteins by 15d-PGJ2

AccNr	Name	control	15-PGJ2	Δ	SM-Scor	Fraction
P11142	Heat shock cognate 71 kDa protein	34	19	*−15*	565.32	C, S, N
P08238	Heat shock protein HSP 90-beta (HSP 90) (HSP 84)	33	18	*−15*	528.87	C, S, N
P07900	Heat shock protein HSP 90-alpha (HSP 86)	33	20	*−13*	544.13	C, S, N
P11021	78 kDa glucose-regulated protein (GRP 78)	23	13	*−10*	365.75	C, S, N
P17987	T-complex protein 1 subunit alpha (TCP-1-alpha)	20	10	*−10*	320.94	C, N
P49368	T-complex protein 1 subunit gamma (TCP-1-gamma) (CCT-gamma) (hTRiC5)	15	5	*−10*	230.97	C, N
P10809	60 kDa heat shock protein, mitochondrial (Heat shock protein 60) (HSP-60)	36	28	*−8*	648.87	C, N
P14625	Endoplasmin (Heat shock protein 90 kDa beta member 1)	17	9	*−8*	238.31	C, N
P30101	Protein disulfide-isomerase A3 (Disulfide isomerase ER-60)	11	3	*−8*	154.12	C, N
P48643	T-complex protein 1 subunit epsilon	18	10	*−8*	268.49	C, N
P50990	T-complex protein 1 subunit theta (TCP-1-theta)	17	9	*−8*	249.51	C, N
Q92598	Heat shock protein 105 kDa (Heat shock 110 kDa protein)	15	8	*−7*	219.83	C, N
P78371	T-complex protein 1 subunit beta (TCP-1-beta)	23	16	*−7*	365.17	C, N
P38646	Stress-70 protein, mitochondrial (75 kDa glucose-regulated protein)	13	7	*−6*	201.73	C, N
P34932	Heat shock 70 kDa protein 4	15	10	*−5*	240.88	C, N
P04792	Heat shock protein beta-1 (HspB1)(Heat shock 27 kDa protein) (HSP 27)	8	3	*−5*	108.88	C, N
P50991	T-complex protein 1 subunit delta (TCP-1-delta) (CCT-delta) (Stimulator of TAR RNA-binding)	15	10	*−5*	264.13	C, N
Q99832	T-complex protein 1 subunit eta (TCP-1-eta)	16	11	*−5*	253.33	C, N
P61604	10 kDa heat shock protein, mitochondrial (Hsp10)	7	3	*−4*	109.65	C, S, N
P40227	T-complex protein 1 subunit zeta (TCP-1-zeta)	19	15	*−4*	346.23	C, N
P27797	Calreticulin (CRP55) (Calregulin)	5	2	*−3*	81.21	C, N

Table 8.5 (continued)

AccNr	Name	control	15-PGJ2	Δ	SM-Scor	Fraction
P08107	Heat shock 70 kDa protein 1 (HSP70.1) (HSP70-1/HSP70-2)	15	12	*−3*	228.12	C, N
P07237	Protein disulfide-isomerase (PDI)	9	6	*−3*	149.75	C, N
Q58FF8	Putative heat shock protein HSP 90-beta 2	6	3	*−3*	96.45	C, N
Q9NQP4	Prefoldin subunit 4 (Protein C-1)	4	2	*−2*	67.02	C, N
Q99471	Prefoldin subunit 5 (C-myc-binding protein Mm-1)	5	3	*−2*	96.61	C, N
P30040	Endoplasmic reticulum protein ERp29	8	7	*−1*	109.52	C, N
P34931	Heat shock 70 kDa protein 1L	6	5	*−1*	107.92	C, N
P61758	Prefoldin subunit 3	3	2	*−1*	50.65	C, N
P13667	Protein disulfide-isomerase A4	3	2	*−1*	40.84	C, N
Q15084	Protein disulfide-isomerase A6	8	7	*−1*	124.13	C, N
Q96JJ7	Protein disulfide-isomerase TMX3		1	*−1*	11.91	C
Q96MM6	Heat shock 70 kDa protein 12B	1	1	*0*	12.1	N
P17066	Heat shock 70 kDa protein 6	4	4	*0*	70.85	C, N
O60925	Prefoldin subunit 1	1	1	*0*	16.45	C, N
Q9UHV9	Prefoldin subunit 2	4	4	*0*	60.91	C, S, N
O15212	Prefoldin subunit 6	5	5	*0*	64.16	C, N

Chaperones regulated by 5 μM 15d-PGJ2 in A375 melanoma cells after 48 h. The accession numbers are from the Uniprot database. Numbers indicate distinct peptides identified by mass spectrometry. C: cytoplasm, N: nucleous, S: supernatant

may therefore serve as a positive prognostic marker indicating the responsiveness to stroma-targeted therapy in the metastatic stage (IV) of melanoma. Meyer et al. suggested that a remodeling of the tumor stroma might be the main target of PPARγ therapy. The recognition of 15d-PGJ2 as a potential anti-tumor drug raises the question of a more detailed understanding of the acting mechanism.

The enhanced knowledge of molecular mechanisms by 15d-PGJ2 generated by shot gun analysis involving important cellular processes, such as cellular signaling networks, regulation of cell cycle, proliferation, transport, cell migration or tumor-stroma interactions may support the design of patient stratification strategies for rational therapeutic concepts.

The data interpretation was supported by the CPL/MUW-database [18]. The number of proteins are automatically classified and provide a fast overview of the main processes involved [18]. Classification considers common household proteins, cell type-specific proteins as well as proteins related to specific functions and enables to decrease the complexicity of data. By comparison of untreated versus treated melanoma cells we were able to confirm the *in vitro* data of the inhibitory effects of 15d-PGJ2 on proliferation, migration and angiogenesis and to extract further relevant proteins involved in tumor progression.

In line with the observation of a decrease of MMP 2 expression in shotgun analysis (downregulation of 1 peptide after 48 h incubation with 5 μM 15d-PGJ2), we were able to reproduce this downregulation using zymography. This observation supports our argument, that 15d-PGJ2 interferes with the tumor microenvironment.

The identification of less peptides of Hsp90 in 15d-PGJ2-treated A375 compared to untreated cells suggested down-regulation of this protein. Western blot analysis of Hsp90, however, did not support this interpretation. 2D-gel electrophoresis demonstrated a profound change of Hsp protein charge by a pI shift which indicates changes in posttranslational modifications such as phosphorylation.

In addition, western blot analysis showed an upregulation of Hsp56 in 1205Lu. Hsp90 and Hsp56 are known to form complexes playing a role in the intracellular trafficking. Phosphorylation of Hsp56 by CK2 was already demonstrated to influence the formation of the HSP90/HSP56 complex [40]. We propose that the reduction of Hsp90 will lead to an elevation of more unbounded Hsp56.

To strengthen the argument that 15d-PGJ2 might increase Hsp90 phosphorylation and to shed light on the impact of 15d-PGJ2 on the phosphorylation which reflects the activity of the proteins, we performed an IP for phospho-serine followed by shot gun analysis indicating a phosphorylation of several chaperones.

Hsp90 belongs to the best studied molecular chaperones which is required for the stability and function of signaling proteins that promote tumor growth, cell motility and invasion *in vitro* and cancer metastasis *in vivo* [41, 42]. Hsp90 inhibitors exhibit significant anti-neoplastic activity against a broad variety of cancers in preclinical studies, including breast, lung cancer and myeloma as well as melanoma [43, 44]. Thus, blockage of Hsp90 interferes with all anti-cancer mechanisms of 15d-PGJ2 and might be one explanation for the widespread activity of 15d-PGJ2 on tumor progression.

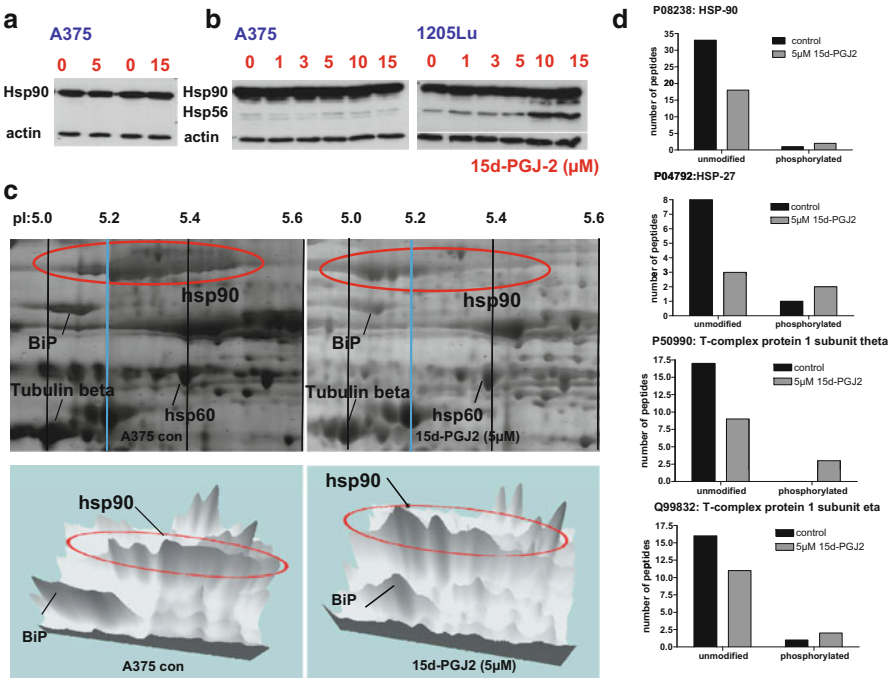

Fig. 8.6 pI shift of Hsp90 in 2D-gel electrophoresis and 15d-PGJ2 induced phosphorylation of several chaperones. **a** Representative immunoblots of three independent experiments of Hsp90 cytosolic (A375) and **b** total cell lysate (A375 and 1205Lu). **c** 2D-gel electrophoresis of 15d-PGJ2 or DMSO treated A375 melanoma cells with additional three dimensional versions. **d** For immunoprecipitation, an anti-phosphoserine antibody was applied to cytoplasmic protein fractions. In case of the four listed chaperones, an apparent down-regulation observed by shotgun proteomics was actually accompanied by phosphorylation as evidenced by increased binding to anti-phosphoserine antibody. Protein abundances were estimated from the number of distinct peptides identified per protein

Verification of these considerations will require further investigation of this drug. The present data allow us to conclude that 15d-PGJ2 interferes with several key mechanism of cancer progression [45], since 15d-PGJ2 potently reduced proliferation of melanoma and melanoma-associated cells, induced apoptosis and cell cycle arrest, and diminished tumor migration, lymphangiogenesis and angiogenesis *in vitro*.

In addition we were able to demonstrate the activity of 15d-PGJ2 on melanoma associated fibroblasts. Tumor-associated stroma cells are known to differ from their normal counterparts in the expression of various biologically molecules such as PPARγ [46], which was found to be upregulated in stromal myofibroblasts of colon adenocarcinomas [47].

Two consequences can be deduced from these results: the evaluation of PPARγ expression in tumor stroma and a correlation with features of melanoma patients would be an interesting approach as proposed by Meyer et al. and 15d-PGJ2 might serve as an efficient combination therapy with chemotherapeutic agents [29, 38].

The IC50 doses to transfer 15d-PGJ2 as a single compound into an *in vivo* situation are high, but we propose that 15d-PGJ2 might serve as an efficient combination therapy with chemotherapeutic agents by targeting as well the tumor microenvironment.

Our data revealed for the first time a profound effect of 15d-PGJ2 on melanoma cells in addition to the tumor microenvironment suggesting high therapeutic efficiency.

Materials and Methods

This study was approved by the "ethics committee of the Medical University of Vienna and the general hospital Vienna" (Ethik-Kommission der Medizinischen Universität Wien und des Allgemeinen Krankenhauses der Stadt Wien AKH, EK-Nr.; 093/2003; EK-Nr.: 1088/2009; EK-Nr.: 1123/2009).

Cell Line and Chemicals

M24met cells (kindly provided by Dr. R.A. Reisfeld, Department of Immunology, Scripps Research Institute, La Jolla, CA; [48] were grown in RPMI 1640 supplemented with 10 % fetal bovine serum, 2 mM glutamine and 50 μg/ml gentamycin sulfate. The human melanoma cell line 1205Lu isolated of a lung metastasis was cultivated as described previously [49]. A375 and Mel Juso were grown in D-MEM tissue culture medium supplemented with 10 % fetal bovine serum, 2 mM glutamine and 50 μg/ml gentamycin sulphate as described previously [50, 51]. Normal human dermal fibroblasts (NHDF) obtained by PromoCell were grown in DMEM (10 % FCS). The compounds used in this study were obtained from Eubio (Vienna, Austria) 15d-PGJ2, ciglitazone, troglitazone and WY-14643. All compounds were resolved in DMSO.

Isolation of Melanoma-Associated Fibroblasts MP9, MP10, MP11 and MCM16

Tumor tissue was digested as described previously [21]. Fibroblasts were magnetically labeled with Anti-Fibroblastic MicroBeads. Cell suspension was loaded onto an MACS Column with a magnetic field. The magnetically labeled fibroblasts were retained within the column and eluted subsequently. Fibroblasts were grown in DMEM (10 % FCS). We obtained written informed consent for collecting excised melanocytic lesions of all patients enrolled. This study was approved by the

"ethics committee of the Medical University of Vienna and the general hospital Vienna" (Ethik-Kommission der Medizinischen Universität Wien und des Allgemeinen Krankenhauses der Stadt Wien AKH, EK-Nr.; 093/2003; EK-Nr.: 1088/2009).

Isolation of HUVECs

HUVECs were isolated from umbilical veins and subcultured as described previously [52]. HUVECs were passaged in IMDM (Life Technologies) containing 10 % FCS (Life Technologies), streptomycin (100 μg/ml), penicillin (100 U/ml), L-glutamine (2 mM), EC growth supplement with heparin (50 μg/ml; Promocell).

Isolation of LECs

Neonatal human foreskins were enzymatically digested, the epidermis was removed and dermal cells mechanically released. CD34-positive blood vascular endothelial cells (BVECs) were isolated by immunomagnetic purification with an anti-human CD34 antibody (BD Pharmingen, San Diego, CA) conjugated to immunomagnetic beads (Dynal. Lake Success, NY). The remaining CD34-negative cells were incubated with an immunomagnetic beads-conjugated anti-human CD31 antibody (Dynal) to isolate LECs. LECs were seeded onto fibronectin-coated (1 μl/ml; BD Biosciences, Bedford, MA) culture dishes and propagated in a modified endothelial cell basal medium.

The use of endothelial cells (HUVECs and LECs) has been approved by the "ethics committee of the Medical University of Vienna and the general hospital Vienna" (Ethik-Kommission der Medizinischen Universität Wien und des Allgemeinen Krankenhauses der Stadt Wien AKH, EK-Nr.1123/2009). We obtained written informed consent from all patients (in the case of umbilical cords, written informed consent was obtained from the parents) [53].

Phenotypes of BEC and LEC cultures have been described recently [54] The used LECs are immortalized LECs.

Cell Proliferation-Assay

The CellTiter 96® AQ_{ueous} Non-Radioactive Cell Proliferation Assay (Promega) was used as previously described [21]. In brief, different cell lines or primary cells were plated and treated with increasing concentrations of 15d-PGJ2 or a solvent control. Proliferation was measured at desired time points employing an ELISA plate reader.

Western Blot

Cells were frozen in liquid nitrogen, lysed and separated by gel electrophoresis as described previously [21, 55]. After blotting membranes were incubated with the following primary antibodies: p21 (1:200), p53ser37 (1:200), p53ser15 (1:200), p53 (1:200), emmprin (basigin) (1:200), Mms2 (1:100), MSH3 (1:500), Hsp90 (1:1000), all Santa Cruz Biotechnology, MSH6 (1:500, Pharmingen) MSH2 (1 μg/ml, Pharmingen), MLH1 (1 μg/ml, Pharmingen) and Nodal (1:500, Abcam), tubulin (mouse anti-tubulin monoclonal antibody, Sigma Aldrich) or actin (rabbit anti-actin monoclonal antibody, Sigma Aldrich). Binding of primary antibodies was visualized by incubation with horseradish peroxidase conjugated secondary antibodies (anti-mouse IgG or anti-rabbit IgG HRP, both GE Healthcare) followed by chemoluminescent visualization with ECL (Amersham).

Cell Cycle Analysis

Cell cycle analysis was performed by propidium iodide FACS staining as described previously [21]. Cells were harvested, and fixed in 70 % ethanol RNase (Sigma) was added, cells stained with propidium iodide and analyzed by flow cytometry. Cell cycle distribution was quantified with the ModFIT LT software (Verity Software House, Topsham, ME).

Matrigel Invasion Chamber Assay

The matrigel invasion chamber assay (BD Biosciences, Bedford, Massachusetts) consists of a two-well chamber system and was peformed as described previously [21]. M24met cells were subjected to different concentrations of 15d-PGJ2 or solvent control. After 48 h, the upper chamber was removed and swiped with a cotton bud. The transmigrated cells on the lower side of the upper chamber were fixed in 70 % ethanol and stained using 0.2 % crystal blue. Pictures were captured with a AxioCam MRc5 digital camera (Zeiss, Vienna, Austria) attached to an AH3-RFCA microscope (Olympus, Vienna, Austria). The relative amount of transmigrated cells was quantified with a computer-assisted analyses system (Axiovision®)

Tube Formation Assay

Matrigel Basement Membrane Matrix (BD) was thawn and 24 well plates were coated with 300 μl Matrigel and incubated for 30 min at 37 °C.

50.000 endothelial cells were seeded and after 8 h different concentrations of 15d-PGJ2 or solvent control were applied. 24 h after seeding tube formation was documented by the confocal laser microscope (Zeiss).

For Calcein staining 12 or 24 h after seeding, cells were washed once with PBS and cells were incubated for 30 min at 37 °C with 50 μL PBS containing 0.05 % Calcein-AM (Sigma Aldrich, Vienna, Austria). Micrographs of fluorescent cells were taken using a Nikon Digital Sight DS-Fi1C CCD camera. Tube formation was quantified using the Cell Profiler Software Package [56]. Briefly, images were converted into binary images by thresholding. Areas with an extension of more than 125 μm in one direction were considered as tubes and selected for analysis, smaller areas were discarded. A single pixel topological skeleton representing the tubular network was constructed and network length was calculated by multiplying the pixel count with a scaling factor representing microns per pixel.

Zymography Assay

We stimulated A375 melanoma cells with increasing doses of 15d-PGJ2 (1, 5, 10, 15 μM) for 48 h. The supernatant was dissolved 1:1 with MTO-buffer (50 mM Tris, pH 7.5; 200 mM NaCl, 5 mM $CaCl_2$) and diluted 1:1 in sample buffer (100 mM Tris-HCl, pH 6.8, 50 % Glycerol, 4 % SDS, 0,1 % Bromphenolblue). The SDS gel contained gelantine (1 mg/ml). After electrophoresis the gel was incubated with substrate buffer with Triton-X100 (50 mM Tris, pH 7.5; 200 mM NaCl, 5 mM CaCl2, 0,02 % Brij; 2.5 % Triton-X100) for 1 h. After incubation substrate buffer without Triton-X100 (50 mM Tris, pH 7.5; 200 mM NaCl, 5 mM CaCl2, 0,02 % Brij) at room temperature (2–3 times/h), the gel was incubated with this buffer over night at 37 °C. Subsequently, the gel was stained in Coomassie solution for 30 min and stripped with a isopropanol-acetic acid solution (ProteaImmun).

Proteome Analysis

Shot gun analysis was performed as described previously [17, 39] In brief, cells were fractionated into nuclear, cytoplasmic and secreted protein fractions [57]. Protein fractions were separated by SDS-PAGE, cut into slices and digested with trypsin. Peptides were extracted and separated by nano-flow LC (1100 Series LC system, Agilent, Palo Alto, CA) using the HPLC-Chip technology (Agilent) equipped with a 40 nl Zorbax 300SB-C18 trapping column and a 75 μm × 150 mm Zorbax 300SB-C18 separation column at a flow rate of 400 nl/min, using a gradient from 0.2 % formic acid and 3 % ACN to 0.2 % formic acid and 40 % ACN over 60 min. Peptide identification was accomplished by MS/MS fragmentation analysis with an iontrap mass spectrometer (XCT-Ultra, Agilent) equipped with an orthogonal nanospray ion source. The MS/MS data were interpreted by the Spectrum Mill MS Proteomics Workbench software (Version A.03.03, Agilent) and searched against the SwissProt Database (Version 14.3 containing 20 328 protein entries) allowing for precursor mass deviation of 1.5 Da, a product mass tolerance of 0.7 Da and a minimum

matched peak intensity (%SPI) of 70 %. Due to previous chemical modification, carbamidomethylation of cysteines was set as fixed modification.

For immunoprecipitation, 5 μg anti-Phosphoserine antibody (PSR-45, Abcam: ab6639) were applied to cytoplasmic protein fractions, followed by an overnight pull-down using Dynal Protein G-coated Dynabeads (Invitrogen). Proteins were released and further processed as described for proteome profiling. In case of the IP analyses, we used a Dionex 3000 nano-LC system and a QEXACTIVE orbitrap mass spectrometer (Thermo). Spectral searches were performed with Mascot.

2D- Gel Electrophoresis

Proteins of A375 melanoma cells treated with 5 μM 15d-PGJ2 or solvent control for 48 h were loaded by passive rehydration of IPG strips pH 5–8, 17 cm (Bio-Rad, Hercules, CA) at room temperature. IEF was performed in a stepwise fashion (1 h 0–500 V linear; 5 h 500 V; 5 h 500–3500 V linear; 12 h 3500 V). After IEF, the strips were equilibrated with 100 mM DTT and 2.5 % iodacetamide according to the instructions of the manufacturer (Bio-Rad Hercules, CA). For SDS-PAGE using the Protean II xi electrophoresis system (Bio-Rad, Hercules, CA, USA), the IPG strips were placed on top of 1.5 mm 12 % polyacrylamide slab gels and overlaid with 0.5 % low melting agarose. The gels were stained with a 400 nM solution of Ruthenium II tris (bathophenanthroline disulfonate) (RuBPS). Fluorography scanning was performed with the FluorImager 595 (Amersham Biosciences, Amersham, UK) at a resolution of 100 μm. After scanning, gels were dried using the slab gel dryer SE110 (Hoefer, San Francisco CA, USA). Exposure of storage phosphor screens (Molecular Dynamics) occurred at room temperature for 24 h. Screens were subsequently scanned using the Phosphorimager SI (Molecular Dynamics) at a resolution of 100 μm. Proteins were identified by mass spectrometry analysis of tryptic digests of isolated protein spots.

Acknowledgments We thank Dr. Ichiro Okamoto and Dr. Oliver Schanab for management of patient sample collection, Dr. Mario Mikula and Dr. Alexander Swoboda for isolation of primary cells, Andrea Holzweber, Editha Bayer, Karin Neumüller and Barbara Pratscher for technical assistance and Johannes Griss for bioinformatic support. We thank DI Thomas Mohr for valuable help with the tube formation assay.

References

1. Schadendorf D (2009) Peroxisome proliferator-activating receptors: a new way to treat melanoma? J Invest Dermatol 129:1061–1063
2. Smalley KS, Herlyn M (2005) Targeting intracellular signaling pathways as a novel strategy in melanoma therapeutics. Ann NY Acad Sci 1059:16–25
3. Nunez NP, Liu H, Meadows GG (2006) PPAR-gamma ligands and amino acid deprivation promote apoptosis of melanoma, prostate, and breast cancer cells. Cancer Lett 236:133–141
4. Schoonjans K, Martin G, Staels B, Auwerx J (1997) Peroxisome proliferator-activated receptors, orphans with ligands and functions. Curr Opin Lipidol 8:159–166

5. Torra IP, Chinetti G, Duval C, Fruchart JC, Staels B (2001) Peroxisome proliferator-activated receptors: from transcriptional control to clinical practice. Curr Opin Lipidol 12:245–254
6. Kihara S, Ouchi N, Funahashi T, Shinohara E, Tamura R et al (1998) Troglitazone enhances glucose uptake and inhibits mitogen-activated protein kinase in human aortic smooth muscle cells. Atherosclerosis 136:163–168
7. Ristow M, Muller-Wieland D, Pfeiffer A, Krone W, Kahn CR (1998) Obesity associated with a mutation in a genetic regulator of adipocyte differentiation. N Engl J Med 339:953–959
8. Kubota T, Koshizuka K, Williamson EA, Asou H, Said JW et al (1998) Ligand for peroxisome proliferator-activated receptor gamma (troglitazone) has potent antitumor effect against human prostate cancer both in vitro and in vivo. Cancer Res 58:3344–3352
9. Mossner R, Schulz U, Kruger U, Middel P, Schinner S et al (2002) Agonists of peroxisome proliferator-activated receptor gamma inhibit cell growth in malignant melanoma. J Invest Dermatol 119:576–582
10. Liu Y, Meng Y, Liu H, Li J, Fu J et al (2006) Growth inhibition and differentiation induced by peroxisome proliferator activated receptor gamma ligand rosiglitazone in human melanoma cell line a375. Med Oncol 23:393–402
11. Goetze S, Eilers F, Bungenstock A, Kintscher U, Stawowy P et al (2002) PPAR activators inhibit endothelial cell migration by targeting Akt. Biochem Biophys Res Commun 293:1431–1437
12. Panigrahy D, Singer S, Shen LQ, Butterfield CE, Freedman DA et al (2002) PPARgamma ligands inhibit primary tumor growth and metastasis by inhibiting angiogenesis. J Clin Invest 110:923–932
13. Placha W, Gil D, Dembinska-Kiec A, Laidler P (2003) The effect of PPARgamma ligands on the proliferation and apoptosis of human melanoma cells. Melanoma Res 13:447–456
14. Smith AG, Beaumont KA, Smit DJ, Thurber AE, Cook AL et al (2009) PPARgamma agonists attenuate proliferation and modulate Wnt/beta-catenin signalling in melanoma cells. Int J Biochem Cell Biol 41:844–852
15. Hoek KS, Schlegel NC, Brafford P, Sucker A, Ugurel S et al (2006) Metastatic potential of melanomas defined by specific gene expression profiles with no BRAF signature. Pigment Cell Res 19:290–302
16. Grabacka M, Plonka PM, Urbanska K, Reiss K (2006) Peroxisome proliferator-activated receptor alpha activation decreases metastatic potential of melanoma cells in vitro via down-regulation of Akt. Clin Cancer Res 12:3028–3036
17. Wimmer H, Gundacker NC, Griss J, Haudek VJ, Stattner S et al (2009) Introducing the CPL/MUW proteome database: interpretation of human liver and liver cancer proteome profiles by referring to isolated primary cells. Electrophoresis 30:2076–2089
18. Haudek-Prinz VJ, Klepeisz P, Slany A, Griss J, Meshcheryakova A, Paulitschke V, Mitulovic G, Stöckl J, Gerner C (2012) Proteome signatures of inflammatory activated primary human peripheral blood mononuclear cells. J Proteomics 76 Spec No.:150–162. doi: 10.1016/j.jprot.2012.07.012. (Epub 2012 Jul 16)
19. Harper JW, Adami GR, Wei N, Keyomarsi K, Elledge SJ (1993) The p21 Cdk-interacting protein Cip1 is a potent inhibitor of G1 cyclin-dependent kinases. Cell 75:805–816
20. Xiong Y, Hannon GJ, Zhang H, Casso D, Kobayashi R et al (1993) p21 is a universal inhibitor of cyclin kinases. Nature 366:701–704
21. Paulitschke V, Schicher N, Szekeres T, Jager W, Elbling L et al (2010) 3,3′,4,4′,5,5′-Hexahydroxystilbene Impairs Melanoma Progression in a Metastatic Mouse Model. J Invest Dermatol 130(6):1668-79. doi: 10.1038/jid.2009.376. Epub 2009 Dec 3.
22. Fievet C, Staels B (2009) Efficacy of peroxisome proliferator-activated receptor agonists in diabetes and coronary artery disease. Curr Atheroscler Rep 11:281–288
23. Bensinger SJ, Tontonoz P (2008) Integration of metabolism and inflammation by lipid-activated nuclear receptors. Nature 454:470–477
24. Lee TS, Tsai HL, Chau LY (2003) Induction of heme oxygenase-1 expression in murine macrophages is essential for the anti-inflammatory effect of low dose 15-deoxy-Delta 12,14-prostaglandin J2. J Biol Chem 278:19325–19330

25. Grommes C, Landreth GE, Sastre M, Beck M, Feinstein DL et al (2006) Inhibition of in vivo glioma growth and invasion by peroxisome proliferator-activated receptor gamma agonist treatment. Mol Pharmacol 70:1524–1533
26. Galli A, Ceni E, Crabb DW, Mello T, Salzano R et al (2004) Antidiabetic thiazolidinediones inhibit invasiveness of pancreatic cancer cells via PPARgamma independent mechanisms. Gut 53:1688–1697
27. Ferruzzi P, Ceni E, Tarocchi M, Grappone C, Milani S et al (2005) Thiazolidinediones inhibit growth and invasiveness of the human adrenocortical cancer cell line H295R. J Clin Endocrinol Metab 90:1332–1339
28. Shen D, Deng C, Zhang M (2007) Peroxisome proliferator-activated receptor gamma agonists inhibit the proliferation and invasion of human colon cancer cells. Postgrad Med J 83:414–419
29. Bundscherer A, Reichle A, Hafner C, Meyer S, Vogt T (2009) Targeting the tumor stroma with peroxisome proliferator activated receptor (PPAR) agonists. Anticancer Agents Med Chem 9:816–821
30. Prakash J, Bansal R, Post E, de Jager-Krikken A, Lub-de Hooge MN et al (2009) Albumin-binding and tumor vasculature determine the antitumor effect of 15-deoxy-Delta-(12,14)-prostaglandin-J(2) in vivo. Neoplasia 11:1348–1358
31. Xin X, Yang S, Kowalski J, Gerritsen ME (1999) Peroxisome proliferator-activated receptor gamma ligands are potent inhibitors of angiogenesis in vitro and in vivo. J Biol Chem 274: 9116–9121
32. Bishop-Bailey D, Hla T (1999) Endothelial cell apoptosis induced by the peroxisome proliferator-activated receptor (PPAR) ligand 15-deoxy-Delta12, 14-prostaglandin J2. J Biol Chem 274:17042–17048
33. Tsuzuki T, Kawakami Y (2008) Tumor angiogenesis suppression by {alpha}-eleostearic acid, a linolenic acid isomer with a conjugated triene system, via peroxisome proliferator-activated receptor {gamma}. Carcinogenesis 29(4):797-806. doi: 10.1093/carcin/bgm298. Epub 2008 Jan 3
34. Funovics P, Brostjan C, Nigisch A, Fila A, Grochot A et al (2006) Effects of 15d-PGJ(2) on VEGF-induced angiogenic activities and expression of VEGF receptors in endothelial cells. Prostaglandins Other Lipid Mediat 79:230–244
35. Dadras SS, Paul T, Bertoncini J, Brown LF, Muzikansky A et al (2003) Tumor lymphangiogenesis: a novel prognostic indicator for cutaneous melanoma metastasis and survival. Am J Pathol 162:1951–1960
36. Shields JD, Borsetti M, Rigby H, Harper SJ, Mortimer PS et al (2004) Lymphatic density and metastatic spread in human malignant melanoma. Br J Cancer 90:693–700
37. Paulitschke V, Kunstfeld R, Gerner C (2010) Secretome proteomics, a novel tool for biomarkers discovery and for guiding biomodulatory therapy approaches. In: From molecular to modular tumor therapy: tumors are reconstructible communicatively evolving systems, vol 3. Springer, pp 405–431
38. Meyer S, Vogt T, Landthaler M, Berand A, Reichle A et al (2009) Cyclooxygenase 2 (COX2) and Peroxisome Proliferator-Activated Receptor Gamma (PPARG) are stage-dependent prognostic markers of malignant melanoma. PPAR Res 2009:848645
39. Paulitschke V, Kunstfeld R, Mohr T, Slany A, Micksche M et al (2009) Entering a new era of rational biomarker discovery for early detection of melanoma metastases: secretome analysis of associated stroma cells. J Proteome Res 8:2501–2510
40. Miyata Y, Chambraud B, Radanyi C, Leclerc J, Lebeau MC et al (1997) Phosphorylation of the immunosuppressant FK506-binding protein FKBP52 by casein kinase II: regulation of HSP90-binding activity of FKBP52. Proc Natl Acad Sci USA 94:14500–14505
41. Tsutsumi S, Neckers L (2007) Extracellular heat shock protein 90: a role for a molecular chaperone in cell motility and cancer metastasis. Cancer Sci 98:1536–1539
42. Powers MV, Workman P (2006) Targeting of multiple signalling pathways by heat shock protein 90 molecular chaperone inhibitors. Endocr Relat Cancer 13(Suppl 1):S125–135
43. Gimenez Ortiz A, Montalar Salcedo J (2010) Heat shock proteins as targets in oncology. Clin Transl Oncol 12:166–173
44. Banerji U (2009) Heat shock protein 90 as a drug target: some like it hot. Clin Cancer Res 15:9–14

45. Hanahan D, Weinberg RA (2000) The hallmarks of cancer. Cell 100:57–70
46. Hofmeister V, Schrama D, Becker JC (2008) Anti-cancer therapies targeting the tumor stroma. Cancer Immunol Immunother 57:1–17
47. Vandoros GP, Konstantinopoulos PA, Sotiropoulou-Bonikou G, Kominea A, Papachristou GI et al (2006) PPAR-gamma is expressed and NF-kB pathway is activated and correlates positively with COX-2 expression in stromal myofibroblasts surrounding colon adenocarcinomas. J Cancer Res Clin Oncol 132:76–84
48. Mueller BM, Romerdahl CA, Trent JM, Reisfeld RA (1991) Suppression of spontaneous melanoma metastasis in scid mice with an antibody to the epidermal growth factor receptor. Cancer Res 51:2193–2198
49. Smalley KS, Brafford P, Haass NK, Brandner JM, Brown E et al (2005) Up-regulated expression of zonula occludens protein-1 in human melanoma associates with N-cadherin and contributes to invasion and adhesion. Am J Pathol 166:1541–1554
50. Schicher N, Paulitschke V, Swoboda A, Kunstfeld R, Loewe R et al (2009) Erlotinib and bevacizumab have synergistic activity against melanoma. Clin Cancer Res 15:3495–3502
51. Hoeller C, Pratscher B, Thallinger C, Winter D, Fink D et al (2005) Clusterin regulates drug-resistance in melanoma cells. J Invest Dermatol 124:1300–1307
52. Petzelbauer P, Bender JR, Wilson J, Pober JS (1993) Heterogeneity of dermal microvascular endothelial cell antigen expression and cytokine responsiveness in situ and in cell culture. J Immunol 151:5062–5072
53. Hoeth M, Niederleithner H, Hofer-Warbinek R, Bilban M, Mayer H et al (2012) The transcription factor SOX18 regulates the expression of matrix metalloproteinase 7 and guidance molecules in human endothelial cells. PLoS ONE 7:e30982
54. Groger M, Niederleithner H, Kerjaschki D, Petzelbauer P (2007) A previously unknown dermal blood vessel phenotype in skin inflammation. J Invest Dermatol 127:2893–2900
55. Hoeller C, Thallinger C, Pratscher B, Bister MD, Schicher N et al (2005) The non-receptor-associated tyrosine kinase Syk is a regulator of metastatic behavior in human melanoma cells. J Invest Dermatol 124:1293–1299
56. Lamprecht MR, Sabatini DM, Carpenter AE (2007) CellProfiler: free, versatile software for automated biological image analysis. Biotechniques 42:71–75
57. Gerner C, Haudek-Prinz VJ, Lackner A, Losert A, Peter-Vorosmarty B et al (2010) Indications for cell stress in response to adenoviral and baculoviral gene transfer observed by proteome profiling of human cancer cells. Electrophoresis 31:1822–1832